Master's Thesis of Science in Agriculture

CRISPR/Cas9 System for Efficient Genome Editing in Filamentous Fungi *Monascus ruber* Based on PacBio SMRT Sequencing

PacBio SMRT 염기서열분석 기술 기반 *Monascus ruber* 대상 CRISPR/Cas9 시스템 개발

August 2021

Hye Ree Yoon

Department of International Agricultural Technology

Graduate School of International Agricultural Technology

Seoul National University

CRISPR/Cas9 System for Efficient Genome Editing in Filamentous Fungi *Monascus ruber* Based on PacBio SMRT Sequencing

A thesis
submitted in partial fulfillment of the requirements to the faculty
of Graduate School of International Agricultural Technology
for the Degree of Master of Science in Agriculture

By
Hye Ree Yoon

Supervised by
Prof. Hyo Jin Kim

Food Technology Major
Department of International Agricultural Technology
Graduate School of International Agricultural Technology
Seoul National University

August 2021

Approved as a qualified thesis
For the Degree of Master of Science in Agriculture
By the committee members

Chairman	Doman Kim, Ph.D.
Vice Chair	Hyo Jin Kim, Ph.D.
Member	Donghwa Chung, Ph.D.

Abstract

The genus *Monascus* has been used in the production of food components, natural pigments, and food supplements with positive effects on human health. As a result of beneficial effects, secondary metabolites produced by *Monascus* spp. have received worldwide attention and used industrially in recent years. It has been proved that *Monascus* spp. can synthesize various secondary metabolites: *Monascus* pigments, monacolin K, and citrinin. *Monascus* pigments have been used as natural food colorants and possess a wide range of biological functions. In addition, monacolin K lowers cholesterol by inhibiting HMG-CoA reductase. Even though *Monascus* spp. produce beneficial secondary metabolites, some strains can secrete citrinin, which has been found to be nephrotoxic, hepatoxic, and carcinogenic. Thus, the *Monascus* fermented food products have been concerned and controversial.

With the advance of fungal metabolic engineering, the formation of secondary metabolites in filamentous fungi could be regulated by genetic engineering. The aim of this study was to establish CRISPR/Cas9 system in *Monascus* spp. based on PacBio SMRT sequencing. In Chapter 2, the whole genome sequence of *Monascus ruber* was generated. The total length of 25.9 Mb was obtained using PacBio RSII sequencer with *de novo* assembly. As a result of genome assemblies with long reads from PacBio SMRT sequencing, the whole genome sequence of *M. ruber* consisted of 13 contigs with 9,639 predicted genes. Furthermore, citrinin biosynthetic gene clusters were mostly lost, while beneficial secondary metabolites, monacolin K and *Monascus* pigments, biosynthetic gene clusters were present in *M. ruber*, indicating this strain serves as a promising industrial strain without citrinin production. To validate *M. ruber* could be characterized as a citrinin-free strain, HPLC analysis was performed and citrinin was not detected

in *M. ruber*. With the genetic analysis of the function of biosynthetic related gene clusters, comprehensive insight into secondary metabolites of *Monascus* spp. was discussed in Chapter 2.

In Chapter 3, CRISPR/Cas9 system was established in *M. ruber* to precisely engineer *MpigI* and *MpigI'*, putative negative transcriptional regulators. *In vitro* transcribed sgRNAs were adopted for transformation in the Cas9 expressed transfomrants to target *MpigI* and *MpigI'*. Based on Sanger sequencing results, six putative mutants were obtained. The mutants generated from the Cas9-mediated cleavage with dual sgRNAs were able to produce increased *Monascus* pigment production compared to the wild-type strain since induced-downregulation of *MpigI* and *MpigI'* leads the increase in *Monascus* pigment production. Further analysis of mutants validated that CRISPR/Cas9 system was successfully established in *M. ruber*. This study was the first report of CRISPR/Cas9 system in *M. ruber.*

Keywords: *Monascus ruber*; *Monascus* pigments; Fungal metabolic engineering; PacBio SMRT sequencing; CRISPR/Cas9 system

Student number: 2019-27916

Contents

List of Tables

Chapter 1

Chapter 2

Chapter 3

List of Figures

Chapter 1

Chapter 2

Chapter 3

Chapter 1.

Research background

1. Fungi

Fungi are a large and diverse group of eukaryotes (Wistreich, 2007). Since many species of fungi can tolerate the wide range of pH and temperature, fungi can live in various environments, such as water, plants, and foods (Frac et al., 2017; Li et al., 2017). Remarkably, fungi play a substantial role as a source of natural product bioactive compound (Alberti et al., 2017). Since the discovery of penicillin in the 1920s, fungal bioactive compounds ranging from antibiotics to statins have been prescribed to save the lives of people (Meyer et al., 2016). These fungal bioactive compounds, termed secondary metabolites, are predominantly produced by filamentous fungi (Keller, 2019).

1.1. Filamentous fungi

Filamentous fungi play vital roles in different industries: pharmaceutical, agriculture, and food (Shi et al., 2017). Because of their considerable economic value of many of their metabolites, filamentous fungi have been widely applied in the production of natural pigments, antibiotics, and cholesterol medications (Dufosse et al., 2014; Nielsen et al., 2017; Shi et al., 2017). Although filamentous fungi produce beneficial secondary metabolites, they can produce other metabolites such as mycotoxins, which can cause harmful or toxic effects on livestock and humans (Salazar-Cerezo et al., 2020).

1.2. *Monascus* spp.

Van Tieghem (1884) firstly screened *Monascus* spp. in red yeast rice and characterized them. The filamentous fungi *Monascus* spp. have been routinely used in the production of fermented foods in eastern Asia (Chen et al., 2015). Their most famous fermented food product is known as red yeast rice, and it has been used as a food supplement to enhance the color and delicacy of meat, fish, and soybean products as part of the Chinese cuisine (Ma et al., 2000). Also, it is recognized as a folk medicine for the rejuvenation of the body and the improvement of blood flow (Zhu et al., 2019). As a result of beneficial effects on human health, the secondary metabolites produced by *Monascus* spp. have received worldwide attention and been used industrially in recent years (Chen et al., 2015). The most common industrial strains are known as *M. ruber, M. purpureus*, and *M. pilosus* (Cheng et al., 2013; Hsu et al., 2011; Lian et al., 2015)

1.3. Red yeast rice

Red yeast rice, termed as *Hongguk* (in Korean) or *Hongqu* (in Chinese), is produced by fermenting the steamed rice with *Monascus* strains (Chen and Hu, 2005). First of all, cooked nonglutinous rice is steamed to a state of semi-gelatinization (Ma et al., 2000). After inoculation of *Monascus* into the rice for fermentation, the rice grains are incubated at 25-28 ℃ and regularly flipped until pigment becomes deep red (Lin et al., 2008). The red yeast rice has been characterized as a folk medicine for improving food digestion and blood circulation (Ma et al., 2000). Previous studies have validated that red yeast rice could lower cholesterol level in blood due to the presence of cholesterol synthase inhibiter, which is known as HMG-CoA reductase (Ma et al., 2000). With the

rising prevalence of hyperlipidemia becomes a worldwide public health concern, *Monascus* fermented products have received more attention than before.

2. Secondary metabolites

2.1. Secondary metabolites in *Monascus* Spp.

It has been proved that *Monascus* spp. can synthesize various secondary metabolites: *Monascus* pigments, monacolin K and citrinin (Chen et al., 2015; Endo 1979; Feng et al., 2012).

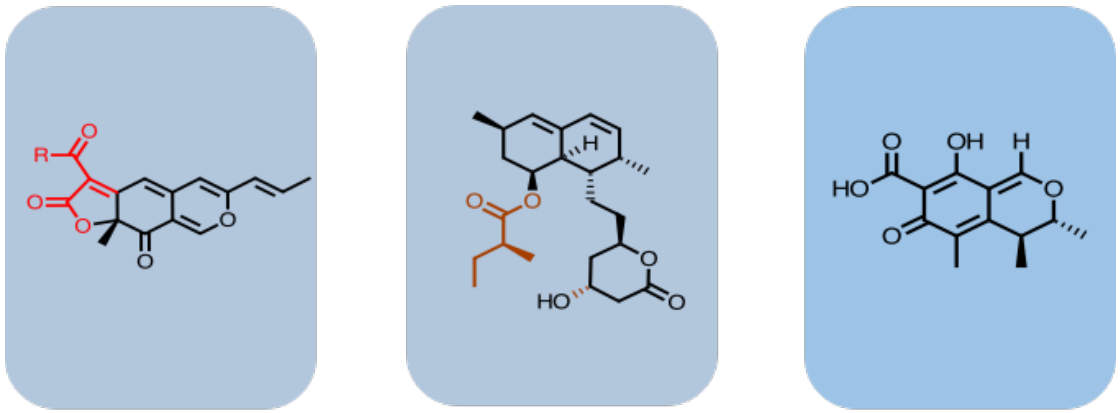

Pigment Monacolin K Citrinin

Fig. 1.1. Secondary metabolites of *Monascus* spp.

2.1.1. *Monascus* pigments

Monascus pigments are polyketide components, also called azaphilones, which are compounds with an oxygenated bicyclic nucleus and a quaternary center (Chen et al., 2015; Kim and Ku, 2018; Patacova, 2013). The main pigments produced by *Monascus* spp. are six compounds: rubropunctamine and monascorubramine (red pigments), rubropunctatin and monascorubrin (orange pigments) and monascin and ankaflavin (yellow pigments) (Kim and Ku, 2018). The orange pigments, rubropunctatin and monascorubrin, are formed by the esterification of polyketide chromophore with beta-ketoacid (from the fatty acid synthase pathway) (Chen et al., 2017; Liu et al., 2018). Then, the red pigments are generated when the orange pigments react with amino group (NH_3) (Chen et al., 2017). In contrast, the yellow pigments are formed by reduction of the orange pigments (Chen et al., 2017). Not only *Monascus* pigments have been used as natural food colorants, but also have several biological functions, leading to antioxidant, antitumor, antimicrobial, antimutagenic properties, and potential antiobesity activities (Chen et al., 2015; Feng et al., 2012). Since the major *Monascus* pigments structurally belong to azaphilones that inhibit other enzyme activities, several beneficial biological functions are available (Patakova, 2013).

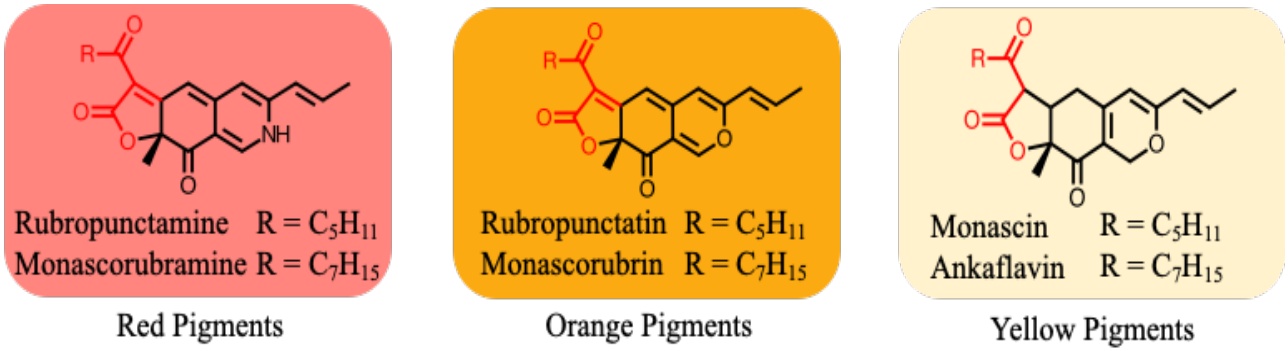

Fig. 1.2. Main pigments produced by *Monascus* spp.

2.1.2. Monacolin K

Endo (1979) firstly isolated monacolin K from the culture of *M. ruber*. Monacolin K (lovastatin) lowers cholesterol by inhibiting HMG-CoA (5-hydroxy-3-methylglutaryl-coenzyme A) reductase, which is known as key and rate liming enzyme for cholesterol synthesis (Klimek et al., 2009). The mechanism of cholesterol synthesis is described in Fig. 1.3.

Cardiovascular diseases, particularly coronary artery disease, are one of the global leading causes of mortality (Liao, 2002). The strong independent predictors of coronary artery disease are increase in total cholesterol, LDL-cholesterol and triglycerides concentrations, as well as decrease in HDL-cholesterol (Lin et al., 2015). Statins, which are widely prescribed class of drugs to lower cholesterol, work by competitively inhibiting the rate limiting enzyme, HMG-CoA reductase, to treat hyperlipidemia (Ward et al., 2019). With the prevalence of hyperlipidemia, *Monascus* fermented food products have been regarded as the hypolipidemic function food, which is having a cholesterol-lowering effect (Lee and Pan, 2012). Lin et al. (2015) reported that *M. purpureus* Went rice significantly reduced LDL-cholesterol, total cholesterol, triglycerides, and apolipoprotein B levels, and well tolerated in patients with hyperlipidemia. Therefore, *Monascus* fermented food product has been validated to lower cholesterol as a functional food.

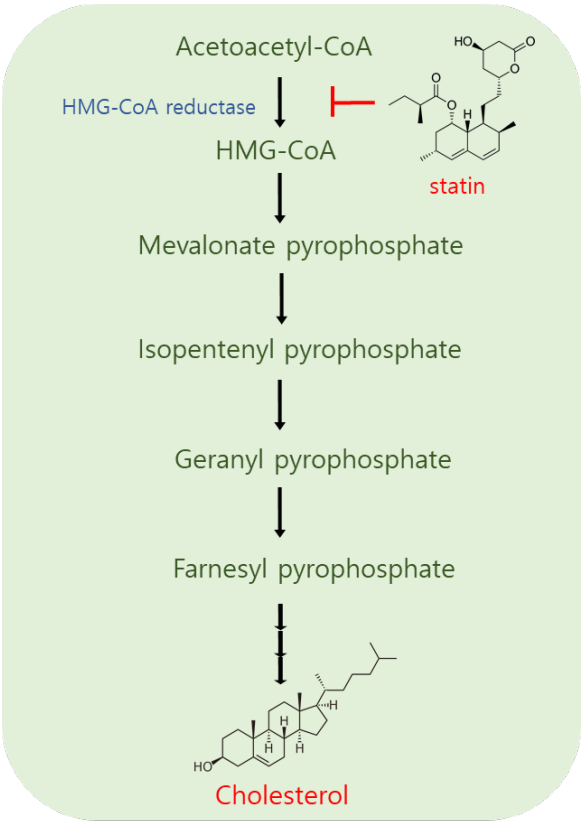

Fig. 1.3. HMG-CoA reductase inhibitor pathway (Slater and Macdonald, 1988).

2.1.3. Citrinin

Even though *Monascus* spp. produce beneficial metabolites and have been used widely in various industries, some strains can secrete mycotoxin citrinin, which was found to be nephrotoxic, hepatoxic, and carcinogenic (Chen et al., 2015; Li et al., 2013). Due to safety concern and controversy over citrinin production in *Monascus* spp., some countries reinforced the restriction on citrinin in *Monascus* fermented products. The European Union countries (2019, November 7) reported that the maximum level of citrinin in food supplements was lowered from 2000 μg/kg to 100 μg/kg based on rice fermented with *Monascus* spp. In eastern Asia, the limit varies in different countries: 50 μg/kg in Korea and 200 μg/kg in Japan (Fu et al., 2007; Kim et al., 2007; Patacova, 2013). Thus, it is important to identify non-citrinin producing strain to be used as promising industrial strain.

3. Genome editing

3.1. Definition and DNA repair pathway

Genome editing enables to manipulate the gene of interest in which DNA is deleted, inserted or replaced via sequence specific manner (Liu et al., 2015; Zheng et al., 2017). The first approach in genome editing begins with introducing double-strand breaks (DSBs) at the target site of specific gene. Since DSBs lead the frequency of homologous recombination, DSBs have been introduced to edit genome in fungal molecular biology artificially and precisely (Krappmann, 2007). When DSBs at the target site of gene take place, damaged DNA is repaired by either non-homologous end joining (NHEJ) pathway or homologous direct recombination (HDR) pathway (Schuster and Kahmann, 2019). The significant difference between two repair pathways is that NEHJ joins DNA without

homology while HDR requires stretches of homologous or homologous sequence (Krappmann, 2007).

3.1.1. Non-homologous end joining (NHEJ) pathway

During NHEJ pathway, nucleotide insertions and deletions (indels) or frameshifts are introduced during the process of repair (Sansbury et al., 2019). In most filamentous fungi, NHEJ is predominant DNA repair mechanism (Schuster and Kahmann, 2019).

3.1.2. Homologous direct recombination (HDR) pathway

During HDR pathway, homologous DNA fragment (donor DNA) to the target sequence is required (Schuster and Kahmann, 2019). Thus, this repair pathway is accomplished by combining Cas9 endonuclease and sgRNA with the transformation of donor DNA (Schuster and Kahmann, 2019).

3.2. CRISPR/Cas9 system

The bacterial immune mechanism CRISPR (Clustered regulatory interspaced short palindromic repeats)/Cas9 system has become a powerful genome editing technology due to its high efficiency with convenience (Nodvig et al., 2015; Pohl et al., 2016; Wang et al., 2018). The two important components are involved in CRISPR/Cas9 system: Cas9 endonuclease and single-guide RNA (sgRNA) (Pohl et al., 2016). The Cas9 is from the bacterium *Streptococcus pyogenes*, and the sgRNA contains a 20-nucleotide sequence (Schuster and Kahmann, 2019). To successfully establish CRISPR/Cas9 system in the target site of genome, both Cas9 endonuclease and the sgRNA should be present in the nuclease (Schuster and Kahmann, 2019). Thus, Cas9 recognizes a protospacer adjacent motif (PAM) sequence and then catalyzes DSBs in the target site (Liu et al., 2015; Shi et al.,

2017). Fig. 1.4 describes the mechanism of CRISPR/Cas9 system with two different DSBs repair pathways

Genetic transformation of fungi meets with many difficulties. Due to complex of cell wall structures, different transformation strategies are required for different fungal species (Li et al., 2017). Several transformation strategies have been employed in filamentous fungi for applying CRISPR/Cas9 system: Poly-ethylene glycol (PEG) mediated transformation, agrobacterium-mediated transformation, and electroporation (Schuster and Kahmann, 2019).

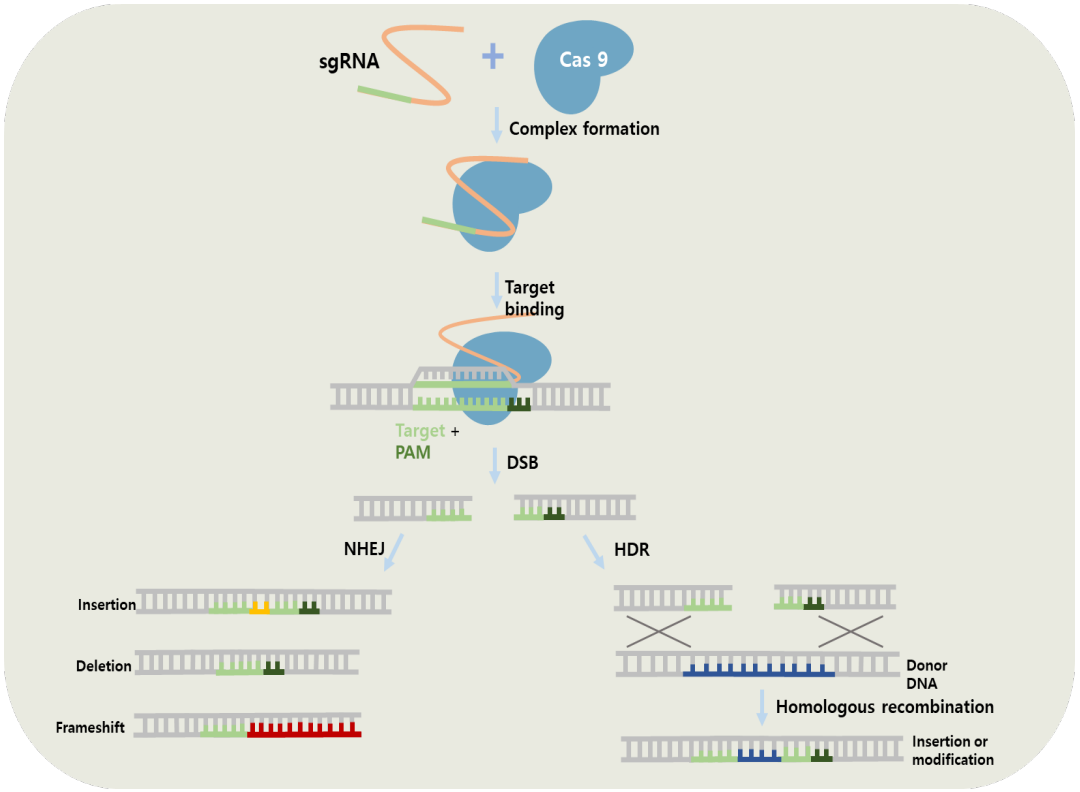

Fig. 1.4. CRISPR/Cas9 system with two different DSBs repair pathways.

3.3. CRISPR/Cas9 system in different species of filamentous fungi

CRISPR/Cas9 system has been established in several filamentous fungi due to their beneficial effects of secondary metabolites on human health, including *Aspergillus spp*., *Fusarium oxysporum*, *Neurospora crassa*, *Penicillium chrysogenum*, *Trichoderma reesei* (Pohl et al., 2016; Schuster and Kahmann, 2019; Wang et al., 2018). Table 1.1. represents currently studied filamentous fungi with CRISPR/Cas9 genome editing system.

Table 1.1. Currently studied filamentous fungi with CRISPR/Cas9 system (Schuster and Kahmann, 2019; Song et al., 2019).

Species	Repair pathway	Application	References
Alternaria alternata	NHEJ	single gene disruption	Wenderoth et al., 2017; Igbalajobi et al., 2019
Aspergillus aculeatus	NHEJ	single gene disruption	Nodvig et al., 2015
Aspergillus brasiliensis	NHEJ	single gene disruption	Nodvig et al., 2015
Aspergillus carbonarius	NHEJ/HDR	single gene disruption	Nodvig et al., 2015; Weyda et al., 2017
Aspergillus fumigatus	NHEJ/HDR	single gene disruption/ multiple gene disruption	Fuller et al., 2015; Weber et al., 2017; Zhang et al., 2016
Aspergillus lucheunsis	NHEJ/HDR	single gene disruption	Nodvig et al., 2015; Nodvig et al., 2018
Aspergillus nidulans	NHEJ/HDR	single gene disruption/ multiple gene disruption	Nodvig et al., 2015; Nodvig et al., 2018
Aspergillus niger	NHEJ/HDR	single gene disruption/ multiple gene disruption	Nodvig et al., 2015; Nodvig et al., 2018
Aspergillus oryzae	NHEJ/HDR	single gene disruption/ multiple gene disruption	Katayama et al., 2015; Nodvig et al., 2018
Beauveria bassiana	NHEJ/HDR	single gene disruption/ multiple gene disruption	Chen et al.,2017
Fusarium fujikuroi	NHEJ/HDR	multiple gene disruption	Shi et al., 2019
Fusarium oxysporum	NHEJ/HDR	single gene disruption	Wang et al., 2018
Mucor circinelloides	NHEJ/HDR	single gene disruption/ multiple gene disruption	Nagy et al., 2017
Myceliophthora thermophila	NHEJ/HDR	single gene disruption/ multiple gene disruption	Liu et al., 2017
Neurospora crassa	NHEJ/HDR	single gene disruption	Matsu-Ura et al., 2015
Penicillium chrysogenum	NHEJ/HDR	single gene disruption	Pohl et al., 2016
Sclerotinia sclerotiorum	NHEJ/HDR	single gene disruption	Li et al., 2018
Talaromyces atroroseus	NHEJ	single gene disruption	Nielson et al., 2017
Trichoderma reesei	NHEJ/HDR	single gene disruption	Liu et al., 2015
Ustilago maydis	NHEJ	single gene disruption/ multiple gene disruption	Schuster et al., 2018

4. Overall objectives

In recent years, perspective on foods has been thoroughly changed. Beyond their nutritional values, foods should provide additional health benefits. Functional foods can promote development and protect against chronic disease risk (Hasler, 2002). Thus, global functional food markets are expected to increase because unhealthy and western food consumption give rise to demand for functional foods (Hasler, 2002).

Monascus fermented food products, especially red yeast rice, caught more attention than ever on account of its validated efficacies to lower cholesterol level and other beneficial effects on human health. However, safety over *Monascus* fermented food product is still concerning and controversial due to citrinin, which limits *Monascus* fermented food products to be consumed. In consequence, it is important to investigate citrinin-free strain to be used as industrial strain.

In Chapter 2, the whole genome sequence of *M. ruber* was obtained using PacBio SMRT sequencing with *de novo* assembly. Based on genome assembly and annotation, the gene clusters of secondary metabolites and biosynthetic pathways were further discussed.

In Chapter3, CRISPR/Cas9 genome editing system was established in *M. ruber*. Interestingly, *M. ruber* possessed two different *MpigI* loci, characterized as putative negative regulators of the biosynthesis of *Monascus* pigments. With this precise genome editing, the target sites of two different *MpigI* (*MpigI* and *MpigI'*) loci were successfully engineered by the Cas9-mediated cleavage with dual sgRNAs and then induced by NHEJ repair pathway.

Chapter 2.

Whole genome sequence of *Monascus ruber* isolated from Korean traditional fermented food

1. Introduction

The history of DNA sequencing began with Fredrick Sanger. Sanger et al. (1977) invented the first generation of DNA sequencing, termed Sanger sequencing, with chain-terminating dideoxynucleotides (ddNTPs). From 1977, Sanger sequencing led to many genetic discoveries and dominated for three decades until emerging Next-generation sequencing (NGS) (Dunn et al., 2018). Compared to Sanger sequencing, NGS was able to sequence large number of genes and entire genome at once (Dunn et al., 2018). Both Sanger sequencing and NGS have been utilizing lately, but high-throughput sequencing has been challenging. Relatively short read length of NGS generated sequences often has resulted assemblies with a large number of contigs (Brede et al., 2020; Smits 2019).

As an alternative, Single Molecule Real Time (SMRT) DNA sequencing, developed by Pacific Biosciences (PacBio), has become the first commercially available for reads that are much longer than NGS or even Sanger sequencing (Chin et al., 2013). Thus, PacBio SMRT sequencing results reduced error rates with long read sequencing since this sequencing utilizes circular consensus sequencing where DNA polymerase repeatedly replicates hairpin-ligated

amplicons, facilitating *de novo* assembly and genome finishing (Whon et al., 2018).

In recent years, there has been substantial attempt to the annotation and sequencing of filamentous fungal genomes (Jones, 2007). Several studies have been reported the whole genome sequence of *Monascus* spp. Liang et al. (2018) reported the complete genome sequence of *M. purpureus* YY-1 and provided the first comprehensive prediction of the biosynthetic pathway of *Monascus* pigments. This study was the first publicly available genome sequence of *Monascus* species and the whole genome sequence of *M. purpureus* YY-1 was sequenced using NGS. Total length of 24.1 Mb was obtained with 7,491 genes in *M. purpureus* YY-1, which was known as one of the most widely used industrial stains for food colorant production in China.

The whole genome of *M. ruber* using PacBio RSII sequencer with high quality *de novo* assembly was generated to obtain trustworthy assembly and annotation in Chapter 2. As a result of genome assemblies with long reads from PacBio SMRT sequencing, the whole genome sequence of *M. ruber* was obtained and annotated. Then, the function of genes involved in secondary metabolites was further analyzed.

2. Materials and methods

2.1. Strain and culture conditions

The strain *M. ruber* was isolated from Korean traditional fermented food, and the strain *M. purpureus* BCRC 31541 was purchased from Bioresources Collection and Research Center (Taipei, Taiwan). Both strains were cultured on potato dextrose agar (PDA) medium at 30 ℃ for hyphae collection. For liquid culture, potato dextrose broth (PDB) medium was used.

2.2. DNA extraction

Genomic DNA of *M. ruber* was extracted through the glass beads method as previously described with slight modifications (Aamir, 2015). The fungal mass obtained from PDA was placed into 2 mL tube containing sterile glass beads and lysis buffer (100 mM Tris HCl pH 8.0, 50 mM EDTA, 3% (w/v) SDS). Tubes containing fungal mass were vortexed vigorously for 20 min. After homogenization process, RNase A was added and incubated at 37 ℃ for 15 min. Then, equal volume of phenol: chloroform: isoamyl alcohol (25:24:1) was added to the supernatant and centrifuged 12,000 rpm for 15 min. The upper aqueous layer was taken, and then equal volume of 100% ethanol was added. The mixture was kept at -20 ℃ for 30 min and centrifuged 12,000 rpm for 10 min. The precipitated DNA pellets were washed with 70% ethanol and dissolved in TE buffer. The quantity and purity of DNA were determined using the NanoVue Plus Spectrophotometer (GE Health Care Co., Nordrhein-Westfalen, Germany) and sent Macrogen (Seoul, Republic of Korea) for sequencing.

2.3. Genomic sequencing and assembly

The sample was prepared according to a protocol for sequencing on the PacBio Sequel system. The DNA templates were sequenced using PacBio RS II sequencer, and *de novo* assembly was performed using CANU (v1.7) software. It was accomplished by mapping single pass reads to seed reads, which represented the longest portion of the read length distribution. Subsequently, a consensus sequence of the mapped read was generated, resulting in long and highly accurate fragments of the target genome. Then, reads were corrected and filtered since some reads did not provide extra information for constructing the genome. In addition, the reads that had too high or too low overlaps were filtered. With the overlapping data, they contained information of each contig, so contigs were constructed with higher quality through the self-mapping step. After complete genome was assembled, the locations of genes were identified. Then, their functions were annotated. Maker (v.2.31.8) was used to predict the location while Protein BLAST+ was performed with UniProt Swiss-Prot (201806).

2.4. Citrinin analysis

Citrinin was analyzed though HPLC as Feng et al. (2014) described. The supernatant was centrifuged for 10 min at 12,000 rpm and then filtered through 0.22 μm membrane filter. HPLC was performed on UltiMate 3000 BioRS system (Thermo Fisher Scientific, Walthan, MA, USA). For stationary phase, the column of inertsil ODS-3 (4.6 mm $\times$ 250 mm, i.d., 5 μm) was used. For mobile phase, a mixture of ACN, water and 0.5% ortho-phosphoric acid in the ratio of 70:25.5:4.5 (v/v/v) was carried out at a flow rate of 0.8 mL/min. The injection volume was 10 μL and the column temperature was set at 30 ℃. The citrinin

contents were monitored by a fluorescence detector at 331 nm excitation wavelength and at 500 nm emission wavelength.

3. Results and discussion

3.1. Genome sequence and assembly

The whole genome sequence of *M. ruber* was generated using the PacBio RSII sequencer and *de novo* genome assembly was conducted with CANU (v1.7) software. Table 2.1. represents the general features of whole genome sequence of *M. ruber*. After filtering process, PacBio SMRT long-read sequencing yielded 737,395 reads with an N50 value of 14.9 kb. Overlapping reads that originated from the same region of the genome could be joined together to form contigs. With CANU bioinformatics software, the overall genome assembly was improved while simultaneously reduced runtime (Korean et al., 2015). In consequence, the total length of 25.9 Mb in 13 contigs was generated with GC content of 48.84 %. The N50 value was increased from 14.9. kb to 3.1 Mb, so CANU performed high quality *de novo* assembly using PacBio library preparation. The length of maximum contig was approximately 3.6 Mb and average length of contigs was about 2.0 Mb. As a result, the consensus sequence with higher quality was generated. The assembly results were summarized in table 2.2.

After genome was analyzed, the locations of protein genes were predicated, and function were annotated. Maker (v2.31.8) was performed to predict the location while protein BLAST+ (v2.6.0) was performed with UniProt Swiss-Prot (201806). The total number of 9,639 genes were predicted and annotated. For RNA, 154 tRNAs, and 41 rRNAs were predicted.

Table 2.1. General features of *M. ruber* genome.

Attribute	Value
Total length (Mb)	25.9
GC content (%)	48.84
Number of genes	9,639
DNA contigs	13
Contig N50 (bp)	3,185,132
Average contig length (bp)	1,993,001
Maximum contig length (bp)	3,583,328
Minimum contig length (bp)	21,886

Table 2.2. Results of assembly.

Contig name	Length (bp)	GC %	Depth
Contig1	3,583,328	48.7	162
Contig2	3,570,546	49.1	151
Contig3	3,344,543	48.8	153
Contig4	3,185,132	49.2	151
Contig5	2,672,239	49.0	151
Contig6	2,300,501	48.8	157
Contig7	1,932,116	48.8	150
Contig8	1,891,921	49.2	152
Contig9	1,567,545	48.3	153
Contig10	1,494,082	48.3	155
Contig11	317,868	49.2	155
Contig12	27,316	25.8	9673
Contig13	21,886	30.2	22
Total	25,909,023	48.84	163

3.2. Comparison with other publicly available *Monascus* genomes

A few publicly available whole genome sequences of *Monascus* spp. were obtained from NGS in previous studies. According to Liang et al. (2018), *M. purpureus* YY-1 has been widely used in food colorant in China, and genome size of this strain was reported 24.1 Mb with 7,491 genes. Fig. 2.1 represents comparison of *M. ruber* and *M. purpureus* YY-1 genomic locations.

In addition, Higa et al. (2020) reported that genome sizes of *M. pilosus* NBRC4520, *M. purpureus* NBRC4478, and *M. ruber* NCBR4485 were around 24 Mb from Illumina Miseq: 8,647 genes *M. pilosus* NBRC4520, 8,891 genes in *M. purpureus* NBRC4478, and 8,645 genes in *M. ruber* NCBR4485

Among publicly available whole genome sequences of *Monascus* spp., *M. ruber* isolated from Korean fermented traditional food possessed additional number of genes and increase in genome size.

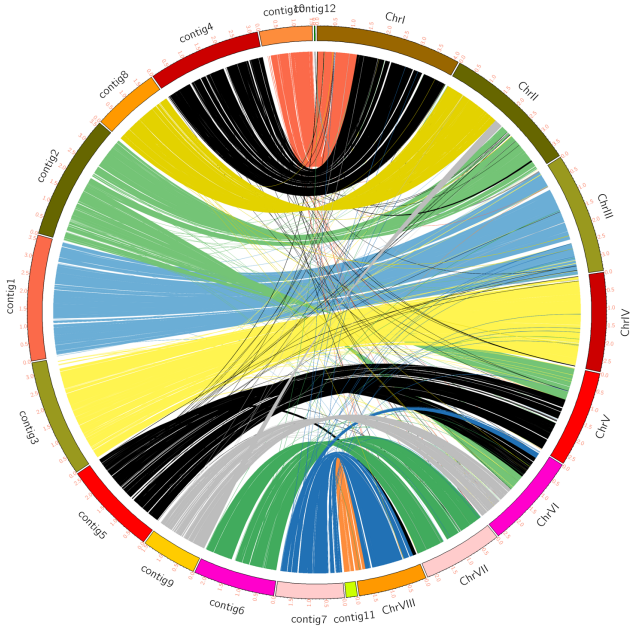

Fig. 2.1. Comparison of *M. ruber* and *M. purpureus* YY-1 genomic locations. The left side of the outer ring depicts the number of contigs in *M. ruber* and the right side of the outer ring depicts the number of chromosomes in *M. purpureus* YY-1. The internal ribbons in different colors connect regions of homologous sequence shared between the two strains.

3.3. Identification of secondary metabolite gene clusters

Table 2.3. represents the gene and function of each gene that are involved in secondary metabolite biosynthesis. With the advantage of PacBio SMRT sequencing, only 13 contigs were assembled in *M. ruber.* In addition, all genes related in secondary metabolite biosynthesis were in contig 2. Two different *MpigI* loci were found from the results of gene annotations, demonstrating two different *MpigI* were present in *M. ruber.* While gene clusters of *Monascus* pigments and monacolin k were present, gene clusters of citrinin were almost lost, suggesting *M. ruber* could be a promising industrial strain without citrinin production.

Table 2.3. Gene annotation information.

contig	Gene ID	Start	End	Strand	Gene	Product	Function
contig 2	LOCUS_001523-RA	490661	496669	+	*MpigJ*	Fatty acid synthase subunit alpha	Pigments biosynthesis
contig 2	LOCUS_001524-RA	496680	498135	-	*MpigI*	Negative regulatory factor	Pigments biosynthesis
contig 2	LOCUS_001525-RA	498265	499088	-	*MpigI*	Negative regulatory factor	Pigments biosynthesis
contig 2	LOCUS_001526-RA	499551	500660	+	*MpigH*	Dehydrogenase	Pigments biosynthesis
contig 2	LOCUS_001527-RA	500771	501592	-	*MpigG*	Oxidoreductase	Pigments biosynthesis
contig 2	LOCUS_001528-RA	501913	503307	-	*MpigF*	Amine oxidase	Pigments biosynthesis
contig 2	LOCUS_001529-RA	503789	504817	+	*MpigE*	Aryl-alcohol dehydrogenase	Pigments biosynthesis
contig 2	LOCUS_001530-RA	504957	506324	-	*MpigD*	3-O-acetyltransferase	Pigments biosynthesis
contig 2	LOCUS_001531-RA	506932	507991	+	*MpigC*	Dehydrogenase	Pigments biosynthesis
contig 2	LOCUS_001532-RA	50814	510123	-	*MpigB*	Transcriptional activator	Pigments biosynthesis
contig 2	LOCUS_001533-RA	512402	520544	+	*MpigA*	Polyketide synthase	Pigments biosynthesis
contig 2	LOCUS_001576-RA	645879	646832	-	*mokC_0*	Dihydromonacolin L monooxygenase mokC	Monacolin K biosynthesis
contig 2	LOCUS_001577-RA	646862	647595	-	*mokC_1*	Dihydromonacolin L monooxygenase mokC	Monacolin K biosynthesis
contig 2	LOCUS_001578-RA	647921	657623	+	*mokA*	Lovastatin nonaketide synthase	Monacolin K biosynthesis
contig 2	LOCUS_001579-RA	658028	658354	-	-	hypothetical protein	
contig 2	LOCUS_001580-RA	661952	662158	+	-	hypothetical protein	
contig 2	LOCUS_001581-RA	662581	663372	-	*mokD*	Esterase mokD	Monacolin K biosynthesis
contig 2	LOCUS_001582-RA	663824	665050	+	*mokE*	Deshydrogenase mokE	Monacolin K biosynthesis
contig 2	LOCUS_001583-RA	665143	666347	-	*lovD_1*	Acyltransferase LovD	Monacolin K biosynthesis
contig 2	LOCUS_001584-RA	667488	670846	-	*mokG*	3-hydroxy-3 methylglutaryl coenzymeA reductase mokG	Monacolin K biosynthesis
contig 2	LOCUS_001585-RA	671858	673272	+	*mokH*	Transcription factor mokH	Monacolin K biosynthesis
contig 2	LOCUS_001586-RA	675002	677151	+	*mokI*	Efflux pump mokI	Monacolin K biosynthesis
contig 2	LOCUS_001587-RA	679695	687775	+	*mokB*	Lovastatin diketide synthase	Monacolin K biosynthesis

3.3.1. *Monascus* pigments biosynthesis

Fig. 2.2 describes a schematic pathway of *Monascus* pigments biosynthesis. The biosynthesis of *Monascus* pigments begin with the condensation of Acetyl CoA and Malonyl-CoA that led the formation of hexaketide chromophore by polyketide synthase (Hajjaj et al., 2000; Chen et al., 2017). *Monascus* pigments are chemical reactions by the esterification of polyketide chromophore with β-ketoacid (Liu et al, 2018). *MpigD,* which encodes 3-O-aetyltransferase, leads the formation of the orange pigments by the esterification (Hajjaj et al., 2000; Chen et al., 2015). It is generally accepted that the reduction reaction of the orange pigments forms the yellow pigments, while the amination reaction of the orange pigments forms red pigments (Chen et al., 2017).

Multiple studies have been conducted the gene clusters of *Monascus* pigments biosynthesis. Liu et al. (2018) found that *MpigA* encoded the polyketide synthase and catalyzed the biosynthesis of key aromatic ring intermediate. Thus, inactivation of *MpigA* (the homolog of *MpKS5*) led an abolishment of pigment and displayed albino phenotype in *M. purpureus* mutant W 13, validating *MpigA* was engaged in pigment production (Balakrishnan et al., 2013). Xie et al. (2013) reported that deletion of *pigR* (*MpigB*) led to the loss of pigment production in *M. ruber* M7, while its overexpression activated a 12-fold higher yield of pigments, suggesting *pigR* was a positive regulator. Liu et al. (2013) found that disruption, complementation, and overexpression of *MpigE* in *M. ruber* M7 had very little effects, and deletion of *MpigE* yielded four kinds of yellow *Monascus* pigments and very little red pigments, suggesting the *MpigE* could be related in the conversion of different pigment compositions.

Biosynthesis of *Monascus* pigments is very complex. Even though several genes related to *Monascus* pigment biosynthesis were manipulated through either disruption or overexpression of the target gene, *MpigI*, a putative negative regulatory factor, was not fully understood while *MpigB*, a positive regulatory factor, was reported in M. *ruber* M7. Therefore, further studies are needed to investigate the function of *MpigI*.

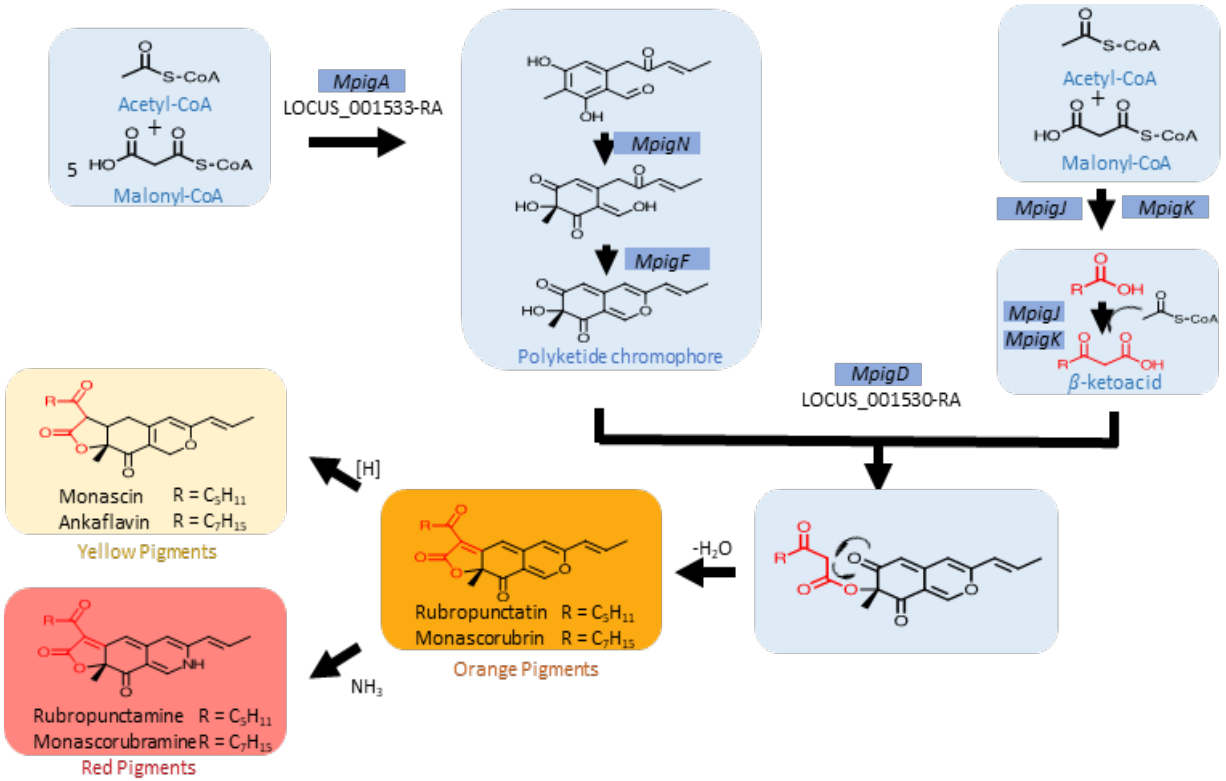

Fig. 2.2. Biosynthetic pathway of *Monascus* pigments. The orange pigments are generated by esterification reaction of polyketide chromophore with β-keoacid. The red pigments are formed by the amination reaction of the orange pigments while the yellow pigments are formed by reduction of the orange pigments.

3.3.2. Monacolin K biosynthesis

Monacolin K, also known as lovastatin, lowers the cholesterol level by inhibiting the HMG-CoA reductase which is the rate limiting step in cholesterol synthesis (Klimek et al., 2009).

Chen et al. (2008) found that disruption in *mokA* led the complete loss of monacolin K production in *M. pilosus* BCRC38072, suggesting that *mokA* was responsible for monacolin k nonaketide synthase. In addition, Sakai et al. (2009) reported that disruption in *mokB* did not produce monacolin K although monacolin J was accumulated in *M. pilosus* NCRC4480, indicating that *mokB* was responsible for biosynthesis of side-chain diketide moiety. Chen et al. (2010) confirmed that transformants showed a 1.7-fold higher yield of monacolin K than the wild-type *M. pilosus* BCRC38072 strain. Monacolin K biosynthetic genes in the transformants were overexpressed than the wild-type through RT-PCR analysis, indicating the *mokH* upregulated the transcription and was responsible for transcription factor.

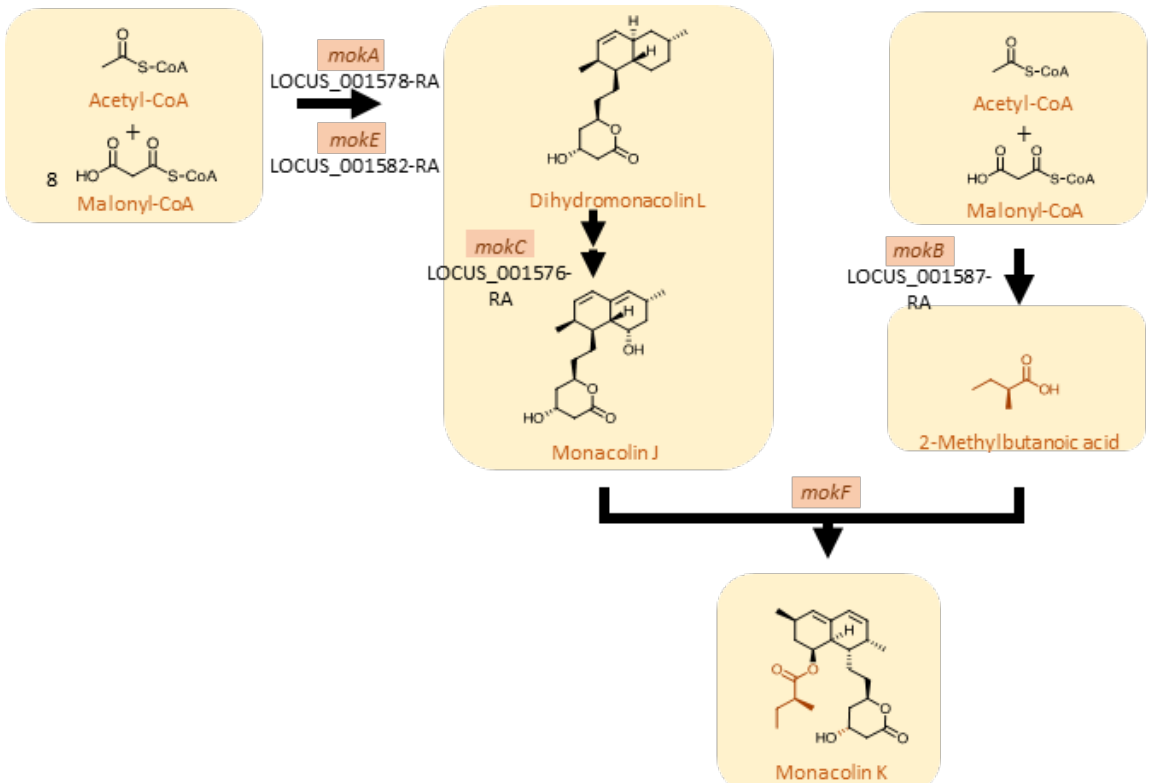

Fig. 2.3. Biosynthetic pathway of monacolin K. Once monacolin J is synthesized, the binding of 2-methylbutanoic acid to monacolin J leads the formation of monacolin K.

3.3.3. Citrinin biosynthesis

According to previous studies, citrinin production was controlled by either optimization of culture condition or application of genetic engineering (Liang et al., 2018). The optimization of culture condition was traditional strategy to control citrinin level, and it was hard to block citrinin production completely (Liang et al., 2018). Thus, manipulation of citrinin biosynthetic related genes could be more practical way to eliminate citrinin concentration by applying genetic engineering. Fig. 2.4 (a) describes the gene clusters of citrinin in *Monascus* spp. Knockout of *pksCT* gene was reported to abolish citrinin biosynthesis in *M. ruber* and *M. purpureus* (Shimizu et al., 2005; Jia et al., 2010; He and Cox 2016).

As shown in Fig. 2.4 (b), citrinin gene clusters of *M. ruber* were mostly lost, and this strongly suggests that *M. ruber* could not be able to produce citrinin during liquid-state fermentation. To validate this, HPLC analysis was performed to detect citrinin and *M. purpureus* strain was used as a control strain. Fig. 2.4 (c) represents the HPLC analysis of *M. ruber* and *M. purpureus* BCRC 31541. While *M. purpureus* BCRC 31541 produced approximately 238.26 ± 15 μg/mL of citrinin on day 18 of cultivation of citrinin, *M. ruber* was not able to produce citrinin. The growth between strain *M. ruber* and *M. purpureus* BCRC 31541 did not have any significant differences. Thus, both results from genome sequence and HPLC analysis demonstrated that *M. ruber* could be served as a promising industrial strain.

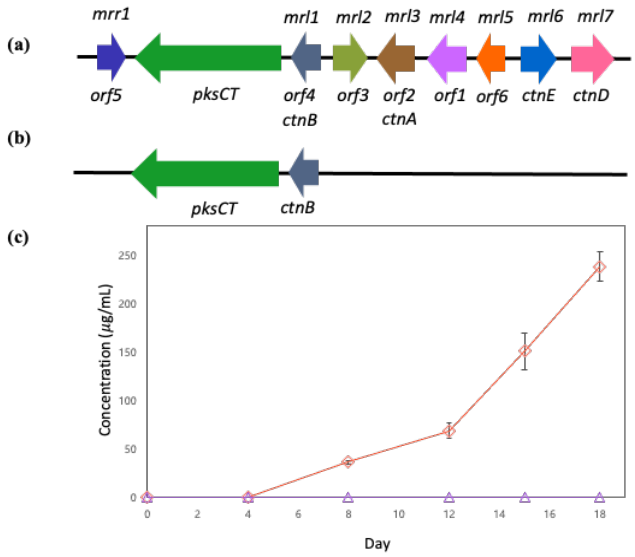

Fig. 2.4. Schematic representation of (a) gene clusters of citrinin in *Monascus* spp. (b) gene clusters of citrinin in *M. ruber* (c) HPLC results of *M. ruber* and *M. purpureus* BCRC 31541. Each plot represents the average of triplicates and error bar depicts the standard deviation.

4. Conclusions

In Chapter 2, the whole genome sequence of *M. ruber* was obtained. Citrinin biosynthetic gene clusters were mostly lost, while beneficial biosynthetic gene clusters of secondary metabolites, monacolin K and *Monascu*s pigments, were present in *M. ruber*. To confirm gene clusters of citrinin were mostly lost in *M. ruber*, HPLC analysis was performed and then citrinin was not detected at all. The results indicated that *M. ruber* could be served as a promising industrial strain without citrinin production.

The total length of 25.9 Mb was generated using PacBio RSII sequencer and *de novo* assembly. This genome consists of 13 contigs with 9,639 predicted genes. With the genetic analysis of gene clusters based on whole genome sequence, secondary metabolites of *M. ruber* was discussed in Chapter 2.

Chapter 3.

CRISPR/Cas9 system in filamentous fungi *Monascus ruber*

1. Introduction

In Chapter 2, gene clusters involved in secondary metabolites of *M. ruber* were studied and discussed. Chapter 2 concluded that citrinin related gene clusters were mostly lost in *M. ruber*, suggesting *M. ruber* could be a citrinin-free strain. According to the results from genome sequence, two different *MpigI* loci were observed in *M. ruber*. In Chapter 3, CRISPR/Cas9 system was employed to precisely manipulate two different *MpigI*, termed *MpigI* and *MpigI'*

Several studies have been conducted to understand the pigment biosynthetic genes in *Monascus* spp. Balakrishnan et al. (2012) reported that *mppR1* (the homologous of *MpigB* in *M. ruber*) and *mppR2* (the homologous of *MpigI* in *M. ruber*) genes in *M. purpureus* were regulatory genes encoded transcription factors for pigment biosynthesis. In addition, Huang et al. (2017) found that H_2O_2 stimulated the pigment production via up-regulation of transcript levels, but *mppR2* was significantly down-regulated and negatively correlated to pigment production. Chen et al. (2015) also reported that the function of *MpigI* was negative regulatory factor. Thus, several studies have been demonstrated the function of *MpigI* could be putative negative regulator, which suppresses the production of pigment, so further studies were necessary to confirm whether *MpigI* suppresses the pigment production or not.

Since filamentous fungi have been proved to produce valuable natural products, CRISPR/Cas9 system has been established in several filamentous fungi, including *Aspergillus spp*., *Fusarium oxysporum*, *Neurospora crassa*, *Penicillium chrysogenum*, *Trichoderma reesei* (Pohl et al., 2016; Schuster and Kahmann, 2019; Wang et al., 2018). Furthermore, CRISPR/Cas9 system has been employed to engineer the pigment production of bikaverin, fungal red pigment with antimicrobial and antitumor activities, in *Fusarium oxysporum*. Wang et al. (2018) reported that *Bik 1* was mutated by using CRISPR/Cas9 system, and introduced mutants were unable to produce the red pigment. This study confirmed that *Bik 1* was responsible for the synthesis of red pigment. Thus, pigment production of secondary metabolite gene cluster in filamentous fungi could be induced by CRISPR/Cas9 system.

In Chapter3, CRISPR/Cas9 system, precise genome editing, was applied to genetically engineer the specific target sites in *M. ruber*. The genes involved in regulation of *Monascus* pigments were manipulated. *Monascus* pigments were widely used as natural food colorants in various industries and possessed several biological functions, leading to antioxidant, antitumor, antimicrobial, antimutagenic properties and potential antiobesity activities. The mutants with increase in *Monascus* pigments could be beneficial to wide range of industries. To increase the *Monascus* pigment production in *M. ruber,* CRIPSR/Cas9 system was employed to inactivate *MpigI* with dual sgRNAs. According to previous studies, gene expression of *MpigI* was downregulated rather than upregulated under cultivation conditions for high pigment production. Thus, CRISPR/Cas9-induced mutations in *MpigI* were expected to upregulate the transcription of pigment biosynthesis. CRISPR/Cas9 system was employed to overproduce *Monascus* pigments by inactivating *MpigI*. Dual sgRNAs were manufactured to

inactivate *MpigI*. After PEG-mediated transformation, randomly selected mutants, and wild-type *M. ruber* strain were compared to validate the increase in pigment production though analysis of secondary metabolites, sequencing, and gene expression.

2. Materials and methods

2.1. Strains, plasmid, primers, and culture conditions

The *Escherichia coli* TOP10 strain (Invitrogen Co, Carlsbad, CA, USA) was served as the general cloning host. The propagation of plasmid was grown in Luria-Bertani (LB) medium at 37 ℃ with 50 μg/ml ampicillin. The strain *M. ruber* was isolated from Korean traditional fermented food, and the strain *M. purpureus* BCRC 31541 was purchased from Bioresources Collection and Research Center (BCRC) in Taiwan. Both strains were cultured on PDA medium at 30 ℃ for hyphae collection. For protoplast regeneration and transformation resistance, molten regeneration medium (0.1% (w/v) yeast extract, 0.1% (w/v) casein enzymatic hydrolysate, 1 M sucrose, 1.6% (w/v) Agar) was prepared for the selection with 200 μg/mL hygromycin B. The plasmid pFC 332 (#87845) containing the Cas9 expressing cassette was purchased from Addgene Inc (Watertown, MA, USA). Primer synthesis were performed by Bioneer Corporation (Daejeon, Republic of Korea), and primers used in this study are listed in table 3.1.

Table 3.1. Primers used in this study.

Primers	Sequence (5' to 3')	Description
F_*M. ruber*	CTCAATGCTTGGTCGTCTCG	random PCR of *M. ruber*
R_*M. ruber*	TGACTACCTCTCTCCGGGAA	
F_cas9 pFC332	GAAGTATAGCATCGGGCTGG	flanking regions of cas9
R_cas9 pFC332	TGACTAAGGTCGATACGGGT	
F_*MpigI*	TCAGCCGTAGCCCAGAGGTG	amplification of *MpigI*
R_*MpigI*	ATGTGGATTGGCCTGCTCTTCG	
F_*MpigI'*	GCAGAAACTGCCTCACCAGG	amplification of *MpigI'*
R_*MpigI'*	ATCTCACTGACCTGCCAGGC	
F_sgRNA 1	TAATACGACTCACTATAGGACTCGACTGCTCCCTCCACAGTTTTAGAGCTAGAA	*in vitro* transcription of sgRNA
F_sgRNA 2	TAATACGACTCACTATAGGGTAAGCGCACCTCTGGGCTAGTTTTAGAGCTAGAA	
F_sgRNA 3	TAATACGACTCACTATAGGTCTCCTCCCTGCTCACACAAGTTTTAGAGCTAGAA	
F_sgRNA 4	TAATACGACTCACTATAGGAGCTCCTTCAAAGCCAGCTGGTTTTAGAGCTAGAA	
R_sgRNA	AGCACCGACTCGGTGCCACTTTTTCAAGTTGATAACGGACTAGCCTTATTTTAACTTGCTATTTCTAGCTCTAAAAC	
F_*MpigI*_del	TTCAGGTAGAGCAGCAGCGT	flanking regions of *MpigI*
R_*MpigI*_del	GGGCAGATTGATCGTCCGAT	
F_*MpigI'*_del	TGGCCGCTGCGAAGGGAATA	flanking regions of *MpigI'*
R_*MpigI'*_del	ATCGTGCACAGCGTGGCATTC	
Oligo dt 18	TTTTTTTTTTTTTTTTTT	cDNA synthesis
GAPDH_F	GAGATCAAGCAGGCCATCAAG	RT-PCR analysis of GAPDH
GAPDH_R	GTAACCCCACTCGTTGTCGT	
F_*MpigI*_RT	AAACACATTCAGCCGTAGCC	RT-PCR analysis of *MpigI*
R_*MpigI*_RT	ATAGGCATGTCGTCGGAAAC	
F_*MpigI'*_RT	GGCGGACATAGGTGCACG	RT-PCR analysis of *MpigI'*
R_*MpigI'*_RT	CAGCAGCAGCTCCTTCAAAG	
F_*MpigA*_RT	CCTGAATGGGTGCAACGAGTAC	RT-PCR analysis of *MpigA*
R_*MpigA*_RT	TATGTACCGCCTCTGCACTG	

2.2. Preparation of *in vitro* transcriptional sgRNA

To efficiently inactivate the target genes, dual sgRNAs were designed to guide Cas9 to simultaneously cleave two sites, spaced 438 bp apart in *MpigI* and 362 bp apart in *MpigI'*. PAM sequence should be present in the 3'end of the target DNA sequence. The 20 nucleotides upstream of PAM sequence (5'-20NGG-3') in *MpigI* and *MpigI'* were designed with the SnapGene Tool. The sgRNA DNA templates were assembled and transcribed by using the MEGAscript T7 kit (Thermo Fisher Scientific, Walthan, MA, USA) according to the manufacture's protocol. Following *in vitro* transcription, enzymatic reactions were purified with MEGAclaer kit (Thermo Fisher Scientific, Walthan, MA, USA). The quantity and purity of sgRNA was measured using the NanoVue Plus Spectrophotometer (GE Health Care Co., Nordrhein-Westfalen, Germany). The purified sgRNAs were stored at -80 ℃, and 100 μg of synthesized sgRNA fragments were transformed into the Cas9 expressed transformants.

2.3. Protoplast preparation and transformation

The PEG-meditated transformation method was followed with slight modifications (Turgeon et al., 2010). The wild-type of *M. ruber* strain was inoculated on PDA and incubated at 30 ℃ for 7 days. Asexual spores (conidia) of the plates were harvested by gently scraping the agar with sterile distilled water. The spores were filtered through 40 μm nylon filter and then filtered spore suspension was inoculated in 100 mL of PDB for 18 h at 30 ℃. The collected mycelia were washed with sterile 0.7 M NaCl. Subsequently, the mycelia were suspended in enzyme solution (0.7 M NaCl, 2% (w/v) Cellulase, 1% (w/v) lysing enzyme and 1% (w/v) Driselase) and then incubated at for 2 h at 30 ℃ with shaking of 80 rpm. Protoplast release was checked every 30 min by microscopic

observation. Released protoplasts were carefully filtered two times, first using sterile Miracloth and then 40 μm nylon filter. Then protoplasts were washed three times with STC buffer (1 M sucrose, 50 mM Tris-HCl and 50 mM $CaCl_2$ pH 8.0). Finally, the protoplasts were resuspended in 500 μL STC buffer and adjusted their density to approximately 10^7-10^8. About 10 μg of linearized plasmid DNA and 100 μg of sgRNAs were added into 100 μL of protoplast suspension and incubated on ice for 20 min. Then, freshly prepared PEG buffer (60% (w/v) PEG 4000, 50 mM Tris-HCl and 50 mM $CaCl_2$ pH 8.0) was added. After transformation, protoplasts were incubated on molten regeneration medium at 30 ℃ for 3-5 days. Finally, transformants were randomly selected and cultured on PDA for further analysis.

2.4. DNA extraction and PCR analysis of putative *M. ruber* transformants

The genomic DNA was extracted same as described in Section 2.2. in Chapter 2. To confirm integration of Cas9, PCR amplification was performed with AccuPower *Taq* PCR premix (Bioneer Co., Daejeon, Republic of Korea) and evaluated though gel electrophoresis. Gene disruption in individual transforments were confirmed by Sanger sequencing.

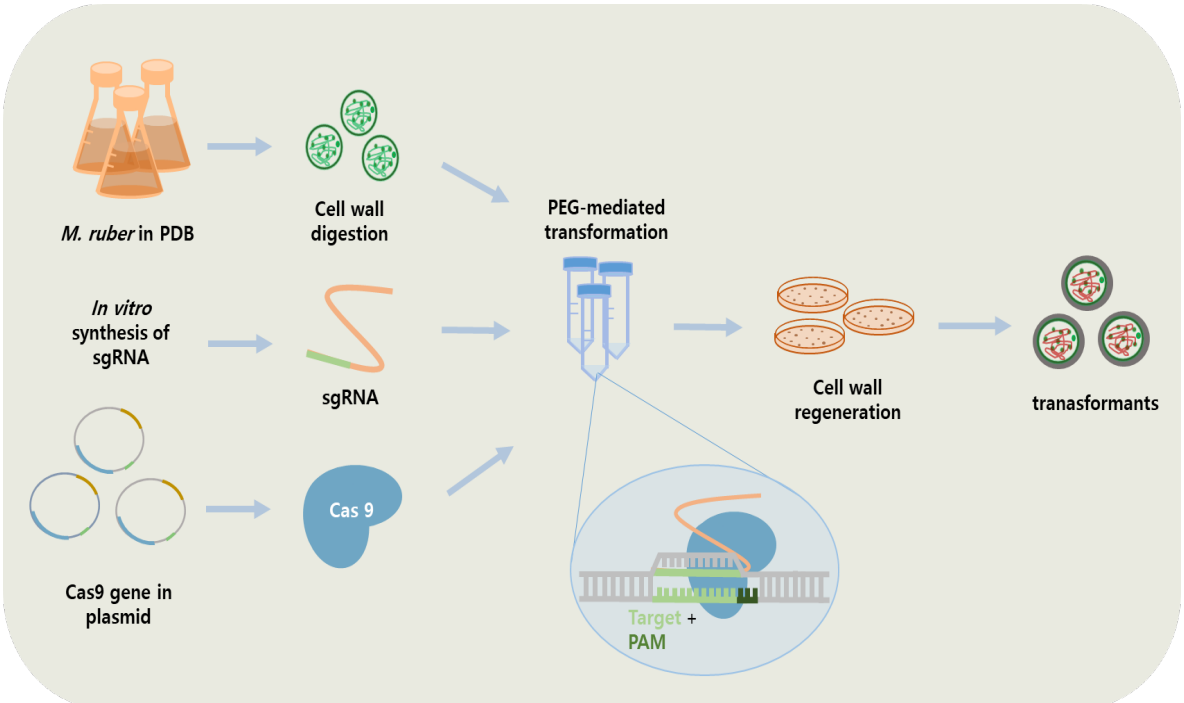

Fig. 3.1. Strategies for the establishment of CRISPR/Cas9 system in *M. ruber*. Cas9 is delivered as plasmid while sgRNA is synthesized following *in vitro* transcription. PEG-mediated transformation method is applied.

2.5. Analysis of secondary metabolites

2.5.1. *Monascus* pigment analysis

The supernatant was removed via centrifugation, and the fermentation samples were taken every 2 days. After filtration, the absorbance of three *Monascus* pigments (yellow, orange, and red) was determined by using UV-1800 spectrophotometer (Shimadzu Co., Kyoto, Japan). Optical density (OD) values at 410, 465, and 505 nm were measured to determine the yields of pigments.

2.5.2. Extraction and analysis of monacolin K

Prior to monacolin K analysis, monacolin K was extracted with minor modifications, according to the previously reported methods (Lin et al., 2018). The wild-type and mutants were inoculated on PDB for 14 days. The mycelium was dried by oven heating at 60 ℃ and finely grounded into powder. Approximately 0.1 g of preparations were extracted with 4 mL of 75% ethanol for 10 min on an ultrasonic bath and subsequently centrifuged at 4200 rpm for 10 min. The supernatant was filtered through 0.22 μm membrane filter. Monacolin K was analyzed though HPLC as previously described (Feng et al., 2014). HPLC was performed on UltiMate 3000 BioRS system (Thermo Fisher Scientific, Walthan, MA, USA). For stationary phase, the column of inertsil ODS-3 (4.6 mm × 250 mm, i.d., 5 μm) was used. For mobile phase, a mixture of ACN, water and 0.5% ortho-phosphoric acid in the ratio of 60:37:3 (v/v/v) was carried out with the flow rate of 1.0 mL/min. The injection volume was 20 μL and the column temperature was set at 25 ℃. The monacolin K contents were monitored by a DAD detector at 237 nm.

2.5.3. Citrinin analysis

Citrinin was analyzed same as described in section 2.4. in Chapter 2.

2.6. RNA extraction and RT-PCR analysis

Mycelia of the wild-type *M. ruber* strain and mutants from 7-day-old cultures were homogenized in liquid nitrogen and grounded into a powder in a pre-chilled mortar and pestle. Then, processed with Universal RNA extraction kit (Bioneer Co., Daejeon, Republic of Korea) following the manufacture's protocol. The quantity and purity of RNA samples were measured using the NanoVue Plus Spectrophotometer (GE Health Care Co., Nordrhein-Westfalen, Germany), and cDNA was synthesized with AccuPower RT premix kit (Bioneer Co., Daejeon, Republic of Korea). For cDNA synthesis, 1 μg of RNA was reverse-transcribed in a 20 μL reaction. GAPDH was used as an internal control, and band intensities of PCR products were compared relative to GAPDH. cDNA synthesis and PCR amplification were performed the following thermocycler conditions: cDNA synthesis at 42 ℃ for 60 min, inactivation of reverse-transcriptase 94 ℃ for 5 min, and amplification of cDNA with 24 cycles of 95 ℃ for 20 s, 60 ℃ for 20 s, and 72 ℃ for 20 s.

3. Results and discussion

3.1. Establishment of Cas9 expressed transformants

Construction of the CRISPR/Cas9 system requires a successful expression of Cas9 in organism. To obtain stable Cas9 expressed transformants, a plasmid, pFC 332, containing *cas9* gene with a SV40 nuclear localization signal (NLS) under the control of *tef1* promoter and terminator from *Aspergillus nidulans* was transformed through PEG-mediated transformation (Nodvig et al., 2015). A stable and viable protoplast formation was the most important factor for PEG-mediated transformation, so yield of protoplasts was frequently observed under microscope. A series of hygromycin-resistant transformants of *M. ruber* was generated. However, since the plasmid pFC 332 lacked a fungus origin of replication, integration of plasmid into the genome could result a cleavage in the *cas9* coding region (Zheng et al., 2017). To confirm the *cas9* coding region was correctly inserted into hygromycin-resistant transformants, PCR amplification using primers flanking the *cas9* coding sequence was performed after PEG-mediated transformation although colonies were grown on antibiotic resistant media. As shown in Fig. 3.2 (a) and (b), eleven of fifteen transformants were confirmed to have 4.1 kb of *cas9* gene correctly integrated into their genome. Among these eleven transformants, randomly selected nine transformants were further investigated to confirm that they belong to *M. ruber* strain. Thus, genomic PCR amplification of 238 bp random sequence of *M. ruber* was performed. As shown in Fig. 3.2 (c) and (d), the Cas9 expressed transformants were able to successfully amplify both 238 bp random genomic DNA sequence and partial 1.1 kb *cas9* sequence while the wild-type strain was only able to amplify 238 bp genomic DNA sequence of *M. ruber*. In addition, plasmid pFC 332 was only able

to amplify partial 1.1 kb of *cas9* sequence. Therefore, stable expression of Cas9 was successfully established in *M. ruber* transformants.

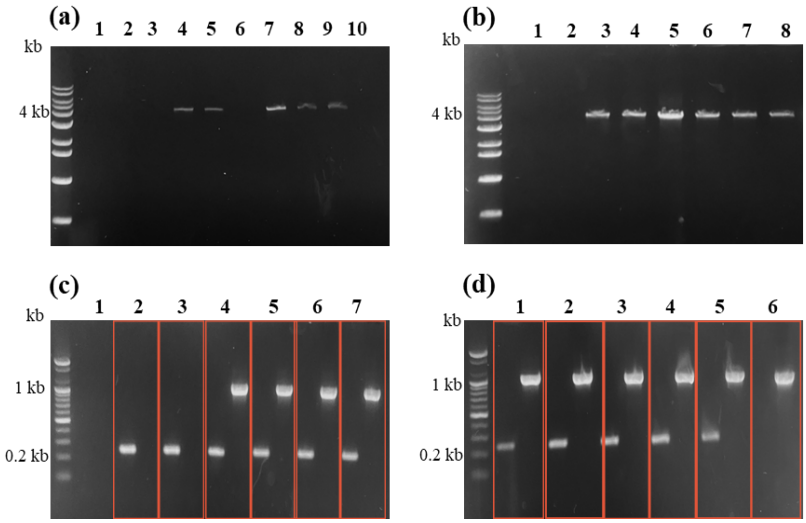

Fig. 3.2. PCR analysis of *cas9* gene integration into the genome. (a) lane 1: H_2O; lane 2 and 3: wild-type; lane 4, 5, 7, 8 and 9: Cas9 expressed transformant. (b) lane 3, 4, 5, 6, 7 and 8: Cas9 expressed transformant. (c) lane 1: H_2O; lane 2 and 3: wild-type; lane 4, 5, 6 and 7: Cas9 expressed transformant. (d) lane 1, 2, 3, 4, and 5: Cas9 expressed transformant; lane 6: plasmid pFC 332.

3.2. Designing dual sgRNA for disrupting *MpigI* and *MpigI'*

In CRISPR/Cas9 system, sgRNA could be delivered though plasmids or as synthetic oligonucleotides. However, vector-based sgRNA system could be laborious to assemble since the construction of multiple vectors, each with different sgRNAs for the different target genes, are required (Ferrara et al., 2019). Thus, in this study, *in vitro* synthesized sgRNAs were adopted for transformation in the Cas9 expressed transformants to target *MpigI* and *MpigI'*. Fig 3.3 (a) represents the gene clusters of *Monascus* pigment (Chen et al., 2015). As discussed earlier, several studies characterized *MpigI* as putative negative transcriptional regulator. To confirm the function of this gene, gene knock out was necessary. The efficiency of inducing mutations using CRISPR/Cas9 system mainly depended on the induction of DSB at the selected target sites (Chen et al., 2014). To efficiently knock out the selected target sites, dual sgRNAs were designed to guide Cas9 to simultaneously cleave two sites, spaced 438 bp apart in *MpigI* and 362 bp apart in *MpigI'*. Fig. 3.3 describes the location of dual target sites of each locus: *MpigI* (b) and *MpigI'*(c). Transformation with dual sgRNAs would be expected to generate DSBs at both target sites resulting in indels, which can be readily detected though PCR amplicons. Hence, the creation of indels with two sgRNAs would knock out the function of gene and then inactivate the suppression of pigment production.

3.3. PCR screening of *M. ruber* Δ*MpigI* and Δ*MpigI'* mutants

The introduced DSBs led to random mutations because of error prone repair mechanism of NHEJ system (Schuster and Kahmann, 2019). The putative transformants were genotyped by PCR amplification of *MpigI* and *MpigI'* coding sequence from genomic DNA using primers flanking both upstream and

downstream cleavage sites, expected size of 1.9 kb in *MpigI* and 1.4 kb in *MpigI'*. As shown in Fig. 3.4 (a) and (b), the resulting PCR amplicons of some transformants showed the shorter length than expected, suggesting some DNA fragments might be deleted in the target regions. Bhattacharya and Van Meir (2019) reported that discriminating the size of PCR products from wild-type and mutants with indels in CRISPR targeted genes could be detected by PCR genotyping. However, most of PCR amplicons were identical to expected size of the wild-type, so sequencing analysis was necessary. These PCR genotyping results allowed a fast method to confirm the indels of the *MpigI* and *MpigI'*. In order to examine the PCR amplicons in further detail, PCR products from putative *MpigI* and *MpigI'* transformants were purified and then subjected to sequencing.

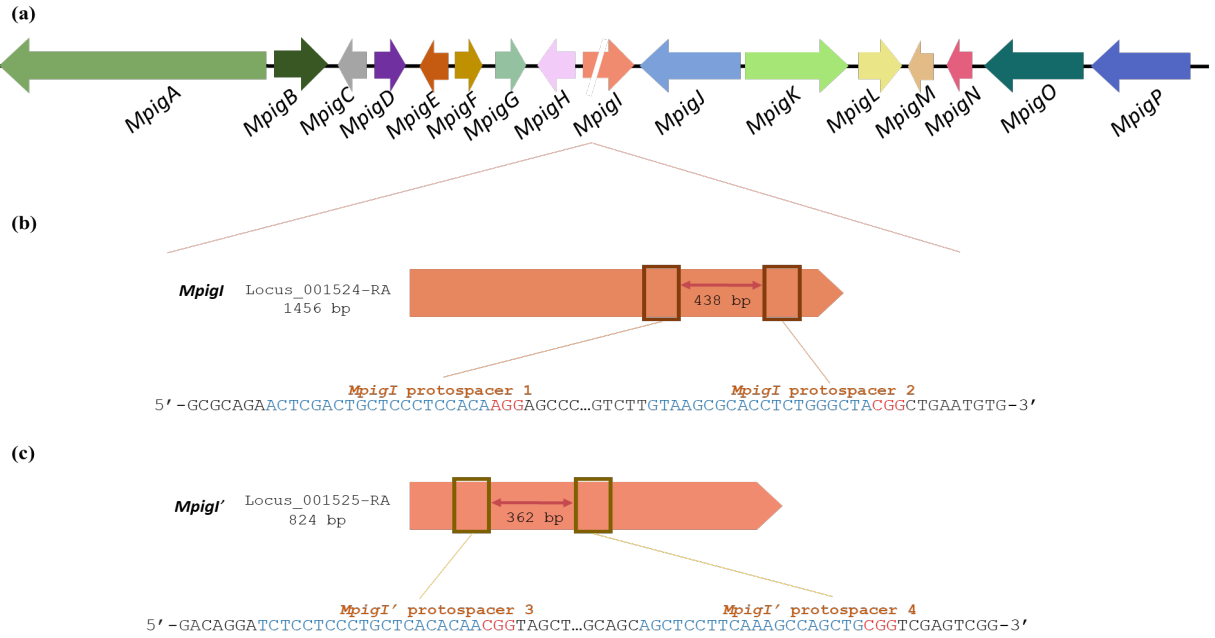

Fig. 3.3. Schematic representation of (a) the gene clusters of *Monascus* pigments and dual target sites in (b) *MpigI* and (c) *MpigI'* loci. Cas9-mediated cleavage of the *MpigI* and *MpigI'* was coupled with dual sgRNAs.

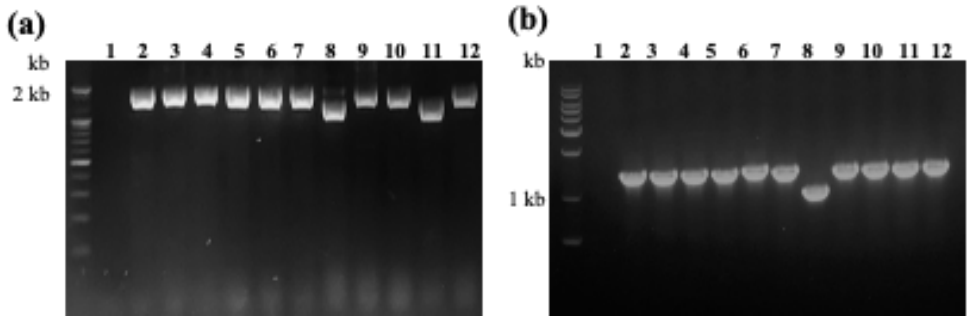

Fig. 3.4. PCR amplification of the target regions in (a) *Mpig I* and (b) *MpigI'* locus using primers flanking the cleavage sites. (a) lane 1: H_2O; lane 2: wild-type; lane 3-12: putative mutants. (b) lane 1: H_2O; lane 2: wild-type; lane 3-12: putative mutants.

3.4. Sequencing analysis of Δ*MpigI* and Δ*MpigI'* mutants

Thirty-five transformants were generated with dual sgRNAs. Based on sequencing results, six putative mutants were obtained: Δ*MpigI16-7*, Δ*MpigI16-15*, Δ*MpigI16-17*, Δ*MpigI16-22*, Δ*MpigI'14-5*, and *MpigI'14-7*.

Fig. 3.5 and 3.6 represent the sequencing chromatogram results of Δ*MpigI16-7* and Δ*MpigI16-15*. The PCR genotyping results of Δ*MpigI16-7* and Δ*MpigI16-15* were identical to the wild-type PCR amplicon. However, when they were subjected to sequencing, nucleotide substitutions were occurred simultaneously between two target sites of *MpigI*, and these nucleotide substitutions caused a single nucleotide insertion when compared with the wild-type sequence.

Fig. 3.7 and 3.8 describe the sequencing chromatogram results of Δ*MpigI16-17* and Δ*MpigI16-22*. The PCR genotyping of Δ*MpigI16-17* and Δ*MpigI16-22* resulted in shorter amplicon, indicating deletion was occurred in target regions. The results from sequencing revealed that 461 bp deletion in Δ*MpigI16-17* and 477 bp deletion in Δ*MpigI16-22*.

Δ*MpigI'14-5* yielded amplicons slightly longer than wild-type PCR amplicon, suggesting some DNA fragments could be inserted at the target site. As shown in Fig. 3.9, sequencing result revealed that 48 bp insertion was introduced at target 3. To determine which DNA fragments were inserted at target 3 of *MpigI'*, the inserted sequence was further analyzed. Interestingly, the inserted sequence was characterized as a sgRNA 4 including sequences of T7 promoter and tracrRNA. Thus, sgRNA 4 was inserted at the target site of sgRNA 3.

The PCR genotyping of Δ*MpigI'14-7* resulted in shorter amplicon compared to the wild- type PCR amplicon, indicating deletion was occurred at target regions. As shown in Fig. 3.10, 385 bp deletion was observed between dual target sites of *MpigI'*.

Sequencing data from mutants revealed the detection of large indels between target sites in both *MpigI* and *MpigI'*. However, a variety of small indels, single nucleotide indels or substitution, at target sites were not observed at this time. Since dual sgRNA system was employed to guide the Cas9 to cleave each target sites, large deletions of DNA sequences between two target sites were detected at this time. Thus, dual sgRNA system would assist the gene knock-out to induce the loss of function. Instead of applying single sgRNA at target site, delivering dual sgRNAs could lead a detection of large indels, so dual sgRNAs optimize the inactivation of target gene.

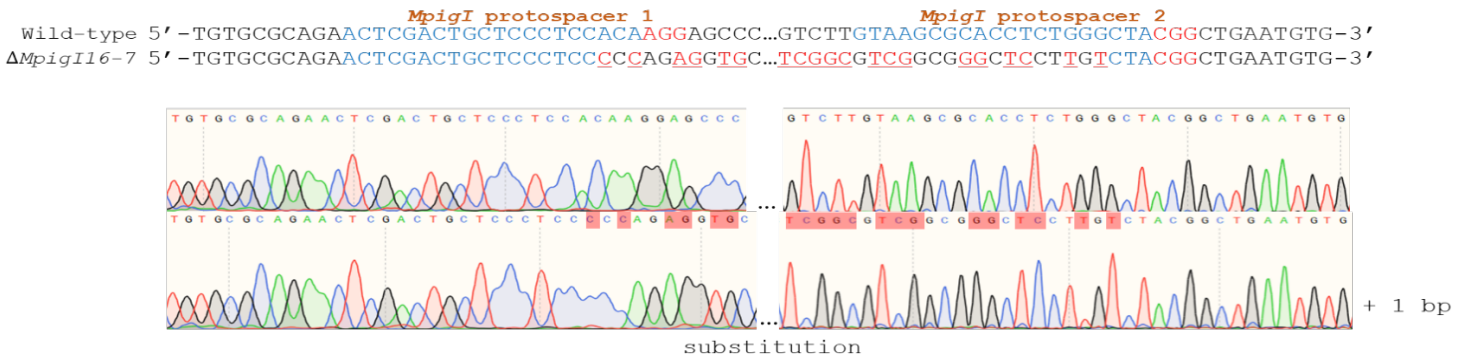

Fig. 3.5. Sequence analysis of the mutant Δ*MpigI16-7*.

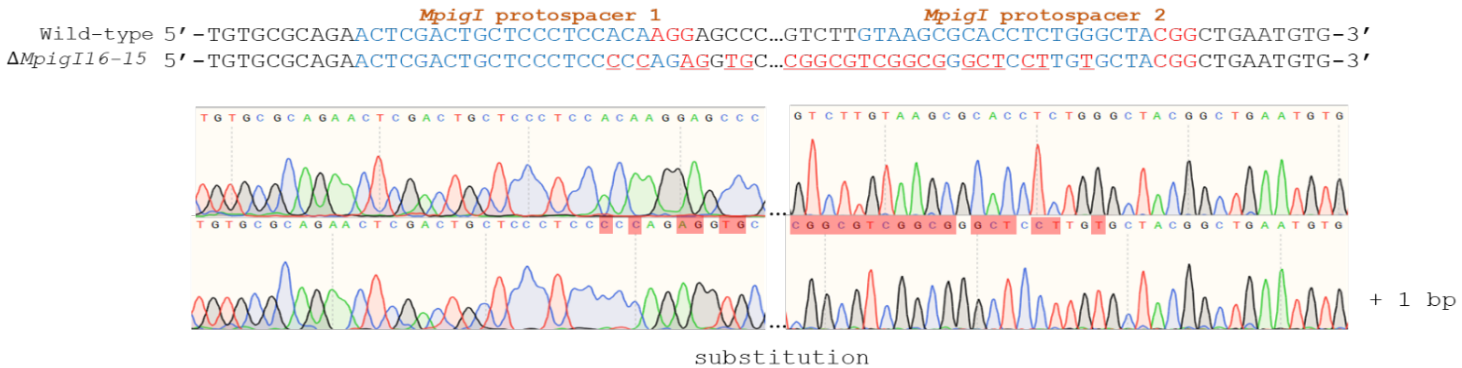

Fig. 3.6. Sequence analysis of the mutant Δ*MpigI16-15*.

Fig. 3.7. Sequence analysis of the mutant Δ*MpigI16-17*.

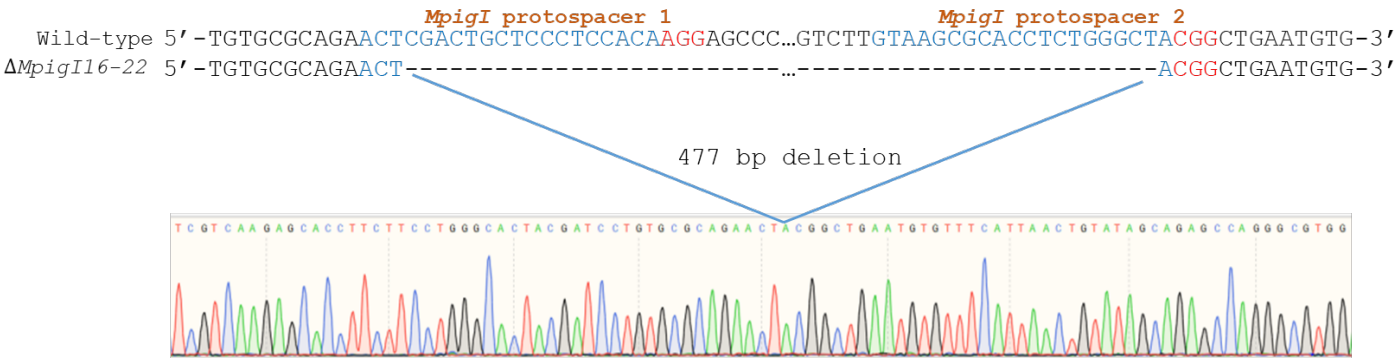

Fig. 3.8. Sequence analysis of the mutant *ΔMpigI16-22*.

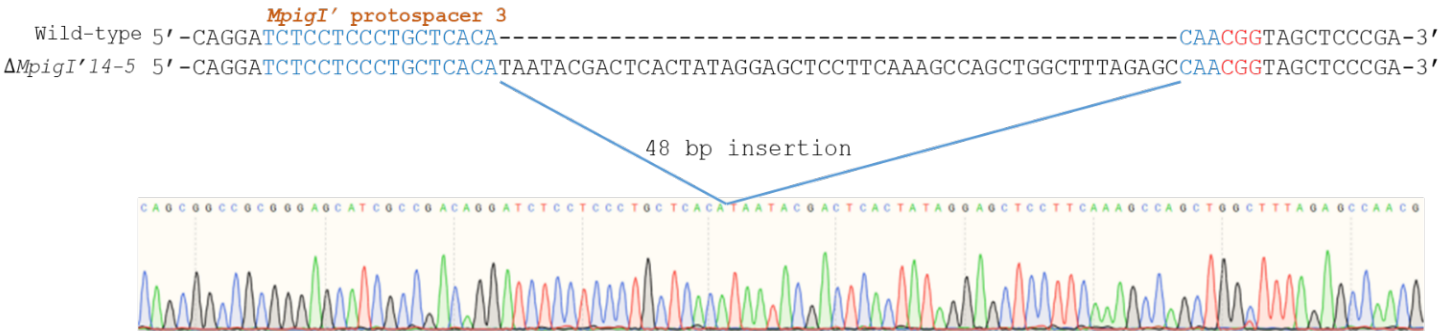

Fig. 3.9. Sequence analysis of the mutant Δ*MpigI'14-5*.

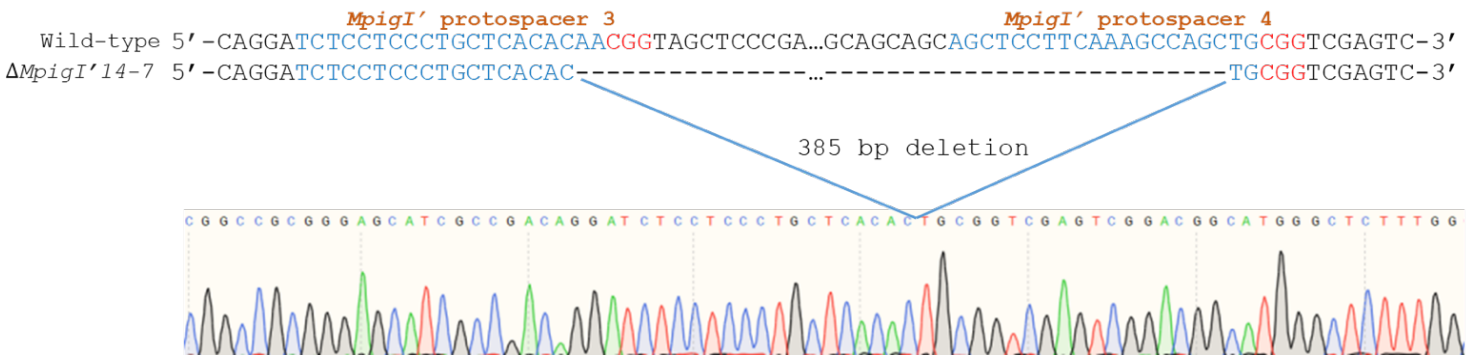

Fig. 3.10. Sequence analysis of the mutant *ΔMpigI'14-7*.

3.5. Comparison of the wild-type *M. ruber* strain and the mutants of Δ*MpigI* and Δ*MpigI'*

3.5.1. Fungal growth

Colony diameter is a reliable indicator of fungal growth. To confirm whether disruption of *MpigI* or *MpigI'* locus would lead to abnormal growth, individual colony of the wild-type *M. ruber* and mutants growing on PDA was measured in every 2 days interval for 14 days. Fig. 3.11 represents the colony diameter. Among the mutants, Δ*MpigI16-15* and Δ*MpigI16-22* showed slightly smaller colony diameter. Besides these two mutants, the other mutants showed similar colony diameter compared to the wild-type *M. ruber* strain. Thus, these results indicated the disruption of *MpigI* or *MpigI'* locus had no significant effect on growth.

3.5.2. Colony morphology

To investigate the resulting phenotypes of mutants, colony morphology of the wild-type *M. ruber* strain and the mutants was analyzed every 4 days interval for 12 days. Fig. 3.12 shows the phenotype of colony in the wild-type *M. ruber* and mutants on PDA. The phenotype of mutants was differed when compared to the wild-type *M. ruber*. Since the function of *MpigI* was reported as a putative negative transcriptional regulator in pigment production, disruption of this gene could inactivate the suppression of pigment production when the Cas9 endonuclease and sgRNA were properly applied in *M. ruber* for targeted genome. Fortunately, this hypothesis was proven correct. The Cas9-mediated cleavage of *MpigI* and *MpigI'* induced the mutants to produce more pigments, indicating the suppression of pigment was inactivated based on CRISPR/Cas9 system. To

examine the *Monascus* pigments in further detail, three main *Monascus* pigments (yellow, orange, and red) were analyzed by using UV-vis spectrophotometer.

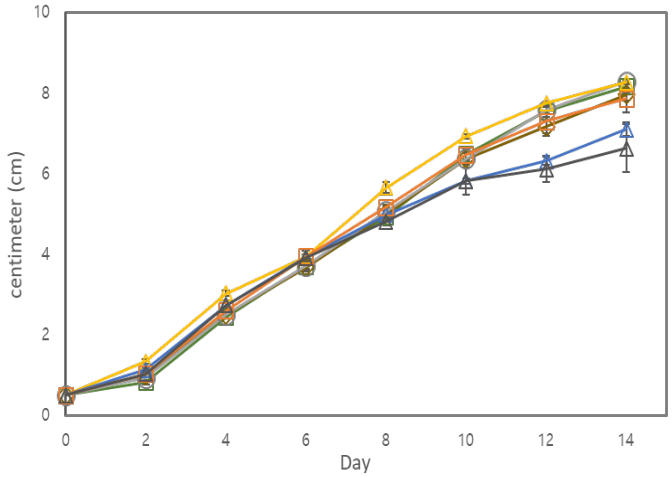

Fig. 3.11. Colony diameter of the wild-type *M. ruber* (green line), Δ*MpigI16-7* (yellow line), Δ*MpigI16-15* (blue line), Δ*MpigI*16-*17* (orange line), Δ*MpigI16-22* (dark gray line), Δ*MpigI'14-5* (khaki line), and Δ*MpigI'14-7* (light gray line). Each plot represents the average of triplicates and error bar depicts the standard deviation.

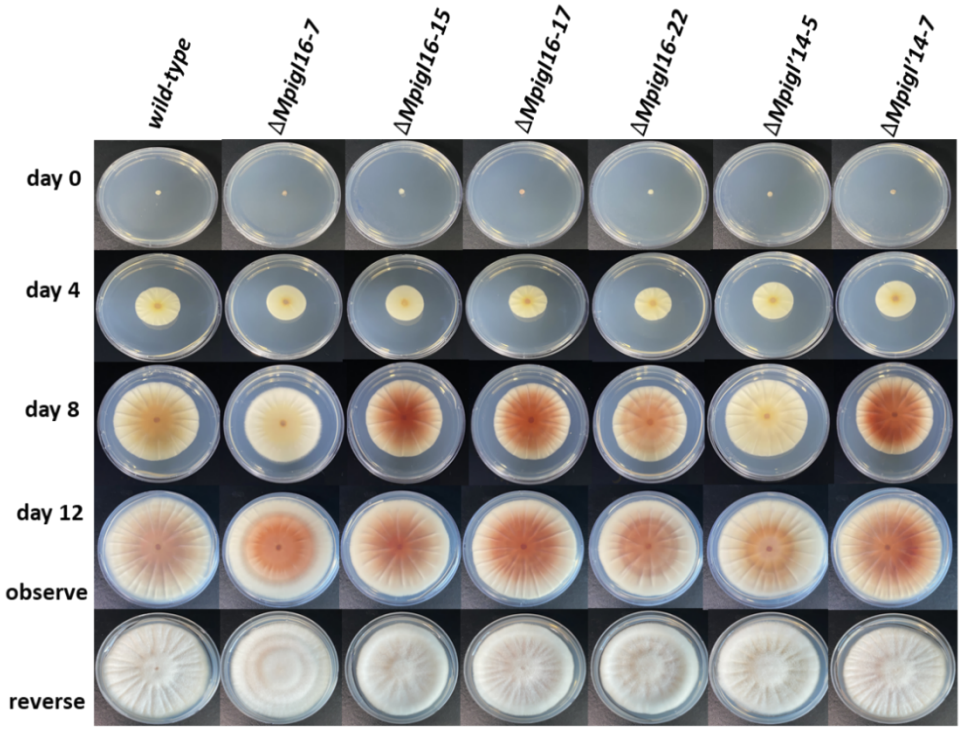

Fig. 3.12. Colony morphology of the wild-type, Δ*MpigI16-7*, Δ*MpigI16-15*, Δ*MpigI16-17*, Δ*MpigI16-22*, Δ*MpigI'14-5*, and Δ*MpigI'14-7*. Measurements were taken every 4 days interval for 12 days in triplicates and figure represents one of these measurements.

3.5.3. *Monascus* pigment production

The production of *Monascus* pigments of the wild-type and mutants was detected in liquid-state fermentation. Three main *Monascus* pigments were measured in every 2 days interval for 14 days. Fig. 3.13 represents (a) yellow, (b) orange, and (c) red pigments produced by the wild-type and mutants.

While the wild-type *M. ruber* mainly produced the yellow pigment, the mutants obtained the ability to generate red and orange pigments with increased yellow pigment. Thus, the Cas9-mediated disruption of *MpigI* and *MpigI'* triggered the mutants to produce more pigments. Apparently, the results from pigment production in liquid-state fermentation were consistent to the results from colony morphology. Among the Δ*MpigI* and Δ*MpigI'* mutants, Δ*MpigI'14-5* (yellow line) produced much less pigment in orange and red than other mutants in liquid-state fermentation. The probable reason for the less pigment production in Δ*MpigI'14-5* could be correlated to the nucleotide insertions at target site. Unlike other mutants, the Cas9-mediated cleavage resulted in small insertion at single target site of Δ*MpigI'14-5,* so the pigment suppression was not completely disrupted. The other mutants established with dual sgRNAs produced much more pigments than wild-type *M. ruber*. Among these mutants, Δ*MpigI*16-*17* (orange line) produced the most pigments than other mutants, and colony morphology of Δ*MpigI*16-*17* proved the phenotype of clear red circle. Thus, the pigment suppression was inactivated, and the function of gene was disrupted by the Cas9-mediated cleavage.

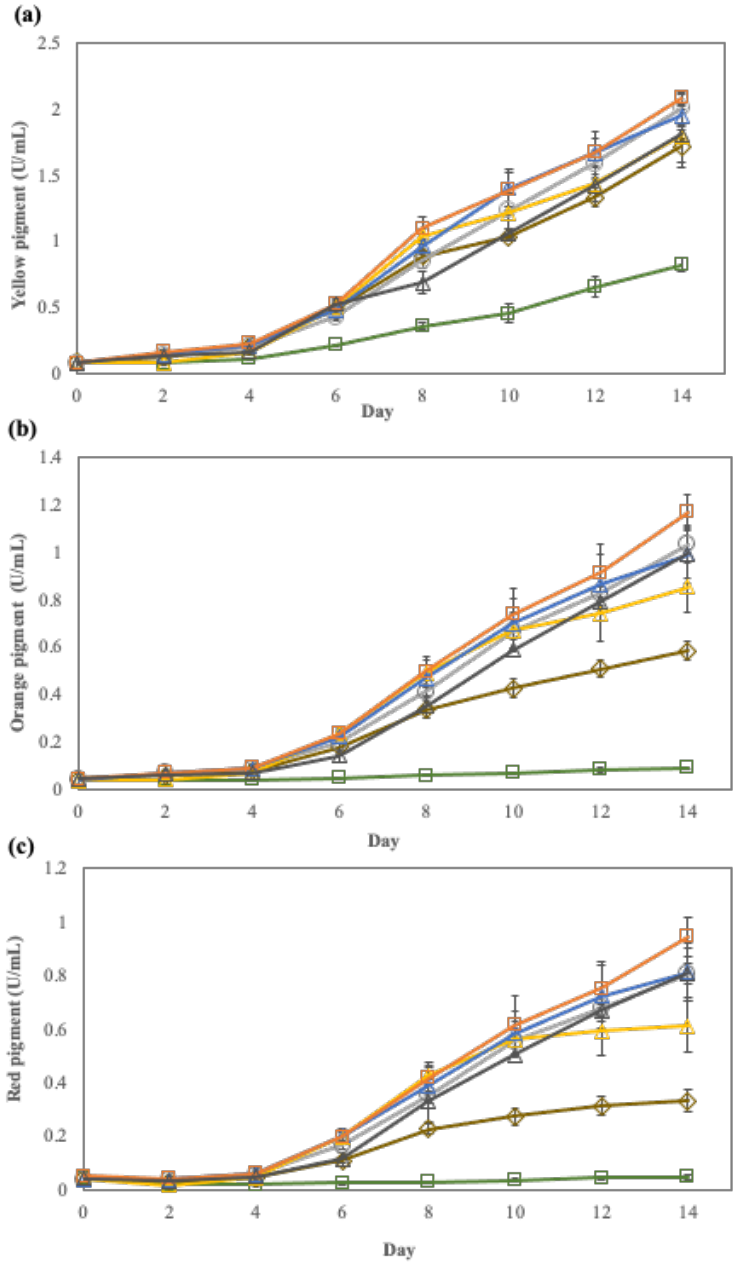

Fig. 3.13. Pigment production of (a) yellow (b) orange, and (c) red pigment of wild-type *M. ruber* (green line), Δ*MpigI16-7* (yellow line), Δ*MpigI16-15* (blue line), Δ*MpigI16-17* (orange line), Δ*MpigI16-22* (dark gray line), Δ*MpigI'14-5* (khaki line), and Δ*MpigI'14-7* (light gray line). Each plot represents the average of triplicates and error bar depicts the standard deviation.

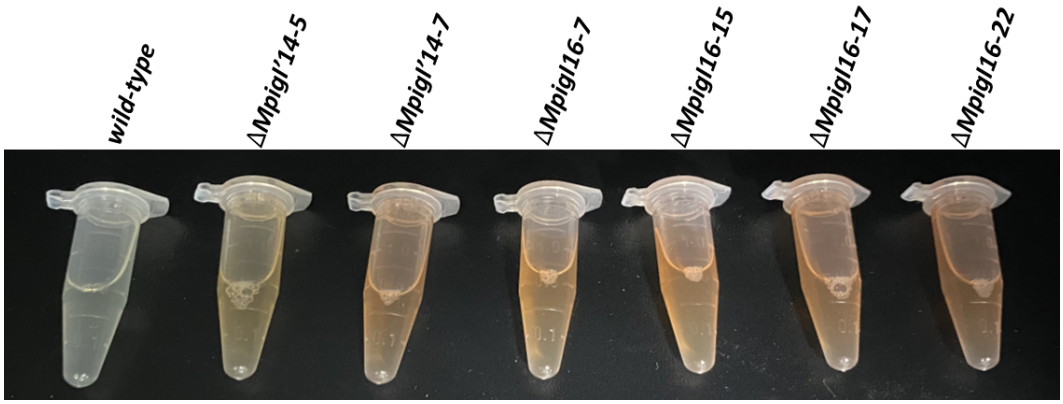

Fig. 3.14. Pigment analysis of wild-type, Δ*MpigI16-7*, Δ*MpigI16-15*, Δ*MpigI16-17*, Δ*MpigI16-22*, Δ*MpigI'14-5, and* Δ*MpigI'14-7.* Measurements were performed in triplicates and figure represents one of these measurements.

3.5.4. Monacolin K analysis

Monacolin K was extracted after 14-day cultivation and then analyzed by using HPLC-UV detector. Both lactone and acid form of monacolin K was found in wild-type and mutants. Fig. 3.15 represents the total amount of monacolin K (a), acid form (b) and lactone form (c) of monacolin K. The wild-type *M. ruber* strain produced 3.52 ± 0.37 μg/mL of monacolin K. Δ*MpigI16-22* and Δ*MpigI'14-5* produced the increased amount of monacolin K comparted to the wild-type *M. ruber* strain. Since all mutants were able to produce monacolin K, the Cas9-mediated cleavage of *MpigI* and *MpigI'* did not cause any negative effects on monacolin K biosynthesis.

3.5.5. Citrinin analysis with *M. purpureus* BCRC 31541

To examine the Cas9-mediated cleavage of *MpigI* and *MpigI'* could affect the citrinin production, the production of citrinin was analyzed by using HPLC-FLD detector. As mentioned in Chapter 2, the results from PacBio SMRT sequencing concluded the gene clusters of citrinin biosynthesis were mostly lost in *M. ruber*. Thus, it was significant to determine the pigment production in mutants although wild-type *M. ruber* strain did not produce citrinin, so *M. purpureus* BCRC 31541 was used as control strain since this strain was reported to produce abundant amount of citrinin. As shown in Fig. 3.16, the wild-type of *M. ruber* did not produce any citrinin whereas *M. purpureus* BCRC 31541 produced 115.6 ± 10.8 μg/mL of citrinin production. In addition, none of the mutants grown under the same condition produced citrinin. Thus, the Cas9-mediated cleavage of *MpigI* and *MpigI'* had no effect on citrinin biosynthesis.

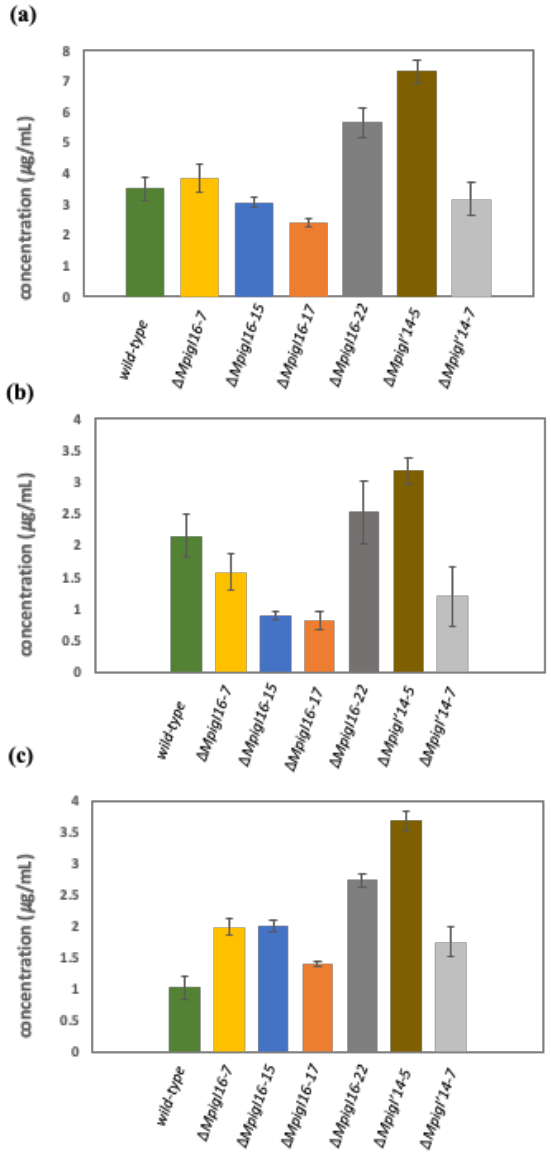

Fig. 3.15. Monacolin K analysis of the wild-type and mutants. (a) total monacolin K (b) acid form and (c) lactone form. Both lactone and acid form of monacolin K were measured through HPLC-UV detector. Each bar plot represents the average of triplicates and error bar depicts the standard deviation.

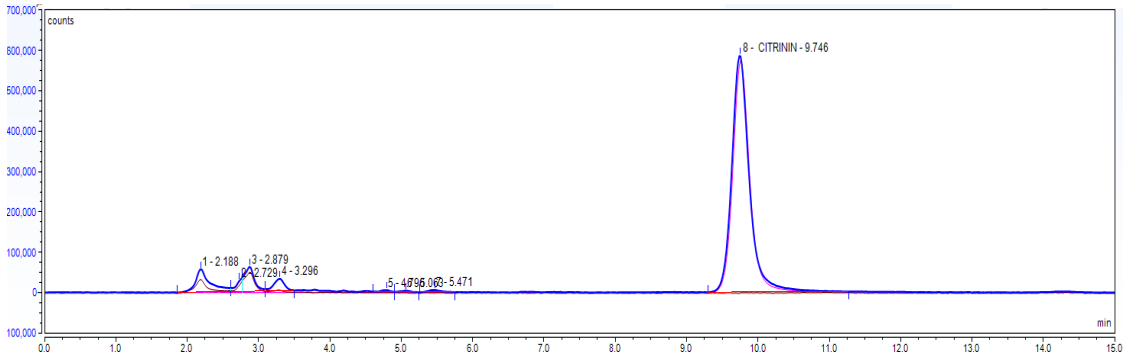

Fig. 3.16. HPLC-FLD chromatograms of wild-type *M. ruber* strain (brown line) and *M. purpureus* BCRC 31541 strain (blue line) compared to standard citrinin 100 µg/mL (pink line). Retention time: 9.746 min. Citrinin measurements were performed in triplicates and figure represents one of these measurements.

3.6. RT-PCR analysis of *MpigI* and *MpigI'* mutants

In order to analyze the expression of *MpigI* and *MpigI'*, total RNA from the wild-type *M. ruber* strain and the mutants of Δ*MpigI* and Δ*MpigI'* were extracted and synthesized to cDNA using oligo-dT primer. Total RNA extracted from the 7-day old culture was used as template in RT-PCR. Fig. 3.17 represents the gel image of RT-PCR amplification resulted in amplification of *MpigA* (polyketide synthase), *MpigI*, *MpigI'*, and glyceraldehyde 3-phosphate dehydrogenase (GAPDH) as an internal control.

As shown in Fig. 3.18, the expression of gene was quantified using gel images. Among the genes associated with *Monascus* pigment production, the Cas9-mediated cleavage of *MpigI* induced downregulation of mutants (Δ*MpigI16-7*, Δ*MpigI16-15*, Δ*MpigI16-17*, Δ*MpigI16-22*). Additionally, the Cas9-mediated cleavage of *MpigI'* induced significant downregulation of *MpigI'14-7*. However, no significant downregulation was found in Δ*MpigI'14-5*, indicating the insertion at single target site was less efficient to inactivate the pigment suppression compared to dual target sites.

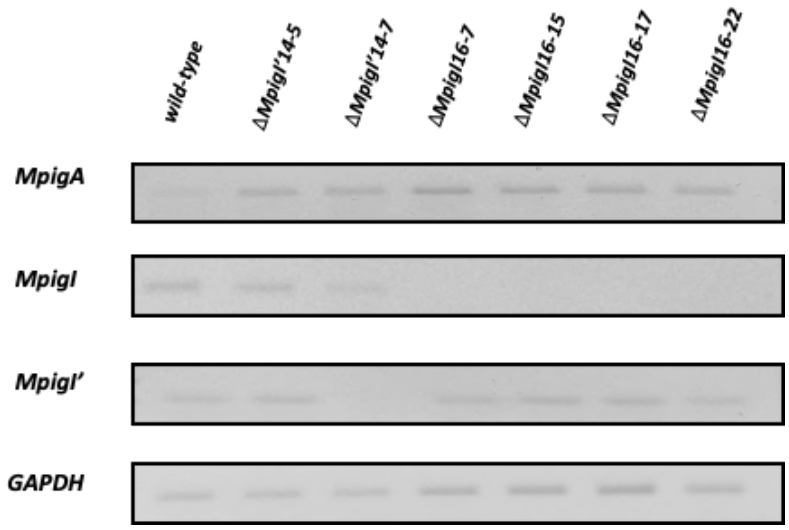

Fig. 3.17. RT-PCR analysis of expression of genes associated with *Monascus* pigments.

4. Conclusions

In Chapter 3, CRISPR/Cas9 system was established in *M. ruber* isolated from Korean traditional fermented food. In vitro transcribed sgRNAs were adopted for transformation in the Cas9 expressed transformants to target *MpigI* and *MpigI'*. Then, the transformants were genotyped by PCR amplification of *MpigI* and *MpigI'* coding sequence from genomic DNA using primers flanking target cleavage sites, and then PCR products were subjected to sequencing. Based on sequencing results, six putative mutants were obtained. The production of *Monascus* pigments was increased by the cleavage of target gene, so induced mutants of Δ*MpigI* and Δ*MpigI'* could be downregulated. In consequence, the use of dual sgRNAs to target each locus were achieved to induce the mutations in both *MpigI* and *MpigI*' via dual sgRNA-directed CRISPR/Cas9 system in *M. ruber*.

CRISPR/cas9 system is known as a powerful and efficient genome editing technology. With this precise genome editing, the suppression of *Monascus* pigment production was appeared to be disrupted by the Cas9-mediated cleavage with dual sgRNAs. This study was the first report of CRISPR/Cas9 system in *M. ruber*, and this new approach of Cas9-mediated cleavage in negative transcriptional regulator will make new comprehensive insight into the biosynthesis pathway and gene regulation.

References

Aamir, S., 2015. A rapid and efficient method of fungal genomic DNA extraction, suitable for PCR based molecular methods. *Plant Pathol Quar*, **5**(2), 74-81.

Ajdari, Z., Ebrahimpour, A., Manan, M. A., Hamid, M., Mohamad, R., Ariff, A. B., 2011. Assessment of Monacolin in the Fermented Products Using *Monascus purpureus* FTC5391. *J. Biomed. Biotechnol*, **2011**, 1-9.

Alberti, F., Foster, G. D., Bailey, A. M., 2017. Natural products from filamentous fungi and production by heterologous expression. *Appl. Microbiol. Biotechnol*, **101**(2), 493-500.

Balakrishnan, B., Karki, S., Chiu, S. H., Kim, H. J., Suh, J. W., Nam, B., Yoon, Y. M., Chen, C. C., Kwon, H. J., 2013. Genetic localization and in vivo characterization of a *Monascus* azaphilone pigment biosynthetic gene cluster. *Appl. Microbiol. Biotechnol*, **97**(14), 6337-6345.

Bhattacharya, D., Van Meir, E.G., 2019. A simple genotyping method to detect small CRISPR-Cas9 induced indels by agarose gel electrophoresis. *Sci Rep* **9,** 4437.

Brede, M., Orton, T., Pinior, B., Roch, F. F., Dzieciol, M., Zwirzitz, B., Wagner, M., Breves, G., Wetzels, S. U., 2020. PacBio and Illumina MiSeq amplicon sequencing confirm full recovery of the bacterial community after subacute ruminal acidosis challenge in the RUSITEC system. *Front. Microbiol,* **11**, 19.

Chen, F. S., Hu, X. Q., 2005. Study on red fermented rice with high concentration of monacolin K and low concentration of citrinin. *Int. J. Food Microbiol*, **103**(3), 331-337.

Chen, G., Bei, Q., Huang, T., Wu, Z. Q., 2017. Tracking of pigment accumulation and secretion in extractive fermentation of *Monascus anka* GIM 3.592. *Microb. Cell. Fact*, **16**, 13.

Chen, J. J., Lai, Y. L., Wang, L. L., Zhai, S. Z., Zou, G., Zhou, Z. H., Cui, C. L., Wang, S. B., 2017. CRISPR/Cas9-mediated efficient genome editing via blastospore-based transformation in entomopathogenic fungus *Beauveria bassiana*. *Sci Rep* **7**, 10.

Chen, W. P., Chen, R., Liu, Q. P., He, Y., He, K., Ding, X. L., Kang, L. J., Guo, X. X., Xie, N. N., Zhou, Y. X., Lu, Y. Y., Cox, R. J., Molnar, I., Li, M., Shao, Y. C., Chen, F. S., 2017. Orange, red, yellow: biosynthesis of azaphilone pigments in *Monascus* fungi. *Chem. Sci*, **8**(7), 4917-4925.

Chen, W. P., He, Y., Zhou, Y. X., Shao, Y. C., Feng, Y. L., Li, M., Chen, F. S., 2015. Edible filamentous fungi from the species *Monascus*: Early traditional fermentations, modern molecular biology, and future genomics. *Compr. Rev. Food. Sci. Food Saf*, **14**(5), 555-567.

Chen, X., Xu F., Zhu, C., Ji, J., Zhou, X., Feng X., Guang S., 2014. Dual sgRNA-directed gene knockout using CRISPR/Cas9 technology in *Caenorhabditis elegans*. *Sci Rep* **4**, 7581.

Chen, Y. P., Tseng, C. P., Liaw, L. L., Wang, C. L., Chen, I. C., Wu, W. J., Wu, M. D., Yuan, G. F., 2008. Cloning and characterization of monacolin K biosynthetic gene cluster from *Monascus pilosus*. *J. Agric. Food Chem*, **56**(14), 5639-5646.

Chen, Y. P., Yuan, G. F., Hsieh, S. Y., Lin, Y. S., Wang, W. Y., Liaw, L. L., Tseng, C. P., 2010. Identification of the *mokH* gene encoding transcription factor for the upregulation of monacolin K biosynthesis in *Monascus pilosus*. *J. Agric. Food Chem*, **58**(1), 287-293.

Cheng, M. J., Wu, M. D., Chen, Y. L., Chen, I. S., Su, Y. S., Yuan, G. F., 2013. Chemical constituents of red yeast rice fermented with the fungus *Monascus pilosus*. *Chem. Nat. Compd*, **49**(2), 249-252.

Chin, C. S., Alexander, D. H., Marks, P., Klammer, A. A., Drake, J., Heiner, C., Clum, A., Copeland, A., Huddleston, J., Eichler, E. E., Turner, S. W., Korlach, J., 2013. Nonhybrid, finished microbial genome assemblies from long-read SMRT sequencing data. *Nat. Methods*, **10**(6), 563-569.

Dufosse, L., Fouillaud, M., Caro, Y., Mapari, S. A. S., Sutthiwong, N., 2014. Filamentous fungi are large-scale producers of pigments and colorants for the food industry. *Curr. Opin. Biotechnol*, **26**, 56-61.

Dunn, P., Albury, C. L., Maksemous, N., Benton, M. C., Sutherland, H. G., Smith, R. A., Haupt, L. M., Griffiths, L. R., 2018. Next generation sequencing methods for diagnosis of epilepsy syndromes. *Front. Genet*, **9**, 11.

Endo, A., 1979. Monacolin-K, a new hypocholesterolemic agent produced by a *Monascus* species. *J. Antibiot*, **32**(8), 852-854.

European Union Law. (2019, November 7). Commission Regulation (EU) 2019/1901. https://eur-lex.europa.eu/eli/reg/2019/1901/oj

Feng, Y. L., Chen, W. P., Chen, F. S., 2016. A *Monascus pilosus* MS-1 strain with high-yield monacolin K but no citrinin. *Food Sci. Biotechnol*, **25**(4), 1115-1122.

Feng, Y. L., Shao, Y. C., Chen, F. S., 2012. *Monascus* pigments. *Appl. Microbiol. Biotechnol*, **96**(6), 1421-1440.

Feng, Y. L., Shao, Y. C., Zhou, Y. X., Chen, F. S., 2014. Monacolin K production by citrinin-free *Monascus pilosus* MS-1 and fermentation process monitoring. *Eng. Life Sci*, **14**(5), 538-545.

Ferrara, M., Haidukowski, M., Logrieco, A. F., Leslie, J. F., Mule, G., 2019. A CRISPR-Cas9 system for genome editing of *Fusarium proliferatum*. *Sci Rep* **9**, 9.

Frac, M., Weber, J., Gryta, A., Debicka, M., Kocowicz, A., Jamroz, E., Oszust, K., Zolnierz, L., 2017. Microbial functional diversity in podzol ectohumus horizons affected by alkaline fly ash in the vicinity of electric power Plant. *Geomicrobiol. J*, **34**(7), 579-586.

Fu, G. M., Xu, Y., Li, Y. P., Tan, W. H., 2007. Construction of a replacement vector to disrupt *pksCT* gene for the mycotoxin citrinin biosynthesis in *Monascus aurantiacus* and maintain food red pigment production. *Asia Pac. J. Clin. Nutr*, **16**, 137-142.

Fuller, K. K., Chen, S., Loros, J. J., Dunlap, J. C., 2015. Development of the CRISPR/Cas9 system for targeted gene disruption in *Aspergillus fumigatus*. *Eukaryot. Cell*, **14**(11), 1073-1080.

Hajjaj, H., Klaebe, A., Goma, G., Blanc, P. J., Barbier, E., Francois, J., 2000. Medium-chain fatty acids affect citrinin production in the filamentous fungus *Monascus ruber*. *Appl. Environ. Microbiol*, **66**(3), 1120-1125.

Hasler, C. M., 2002. Functional foods: Benefits, concerns and challenges-a position paper from the American Council on Science and Health. *J. Nutr*, **132**(12), 3772-3781.

He, Y., Cox, R. J., 2016. The molecular steps of citrinin biosynthesis in fungi. *Chem. Sci*, **7**(3), 2119-2127.

Higa, Y., Kim, YS., Altaf-Ul-Amin, M. *et al.*, 2020. Divergence of metabolites in three phylogenetically close *Monascus* species (*M. pilosus*, *M. ruber,* and *M. purpureus*) based on secondary metabolite biosynthetic gene clusters. *BMC Genomics*, **21**,679.

Hsu, Y. W., Hsu, L. C., Liang, Y. H., Kuo, Y. H., Pan, T. M., 2011. New bioactive orange pigments with yellow fluorescence from *Monascus*-fermented *Dioscorea*. *J. Agric. Food Chem*, **59**(9), 4512-4518.

Huang, T., Tan, H. L., Lu, F. J., Chen, G., Wu, Z. Q., 2017. Changing oxidoreduction potential to improve water-soluble yellow pigment production with *Monascus ruber* CGMCC 10910. *Microb. Cell. Fact*, **16**, 12.

Igbalajobi, O., Yu, Z. Z., Fischer, R., 2019. Red- and blue-light sensing in the Plant pathogen *Alternaria alternata* depends on phytochrome and the white-collar protein *LreA*. *mBio*, **10**(2), 17.

Jia, X. Q., Xu, Z. N., Zhou, L. P., Sung, C. K., 2010. Elimination of the mycotoxin citrinin production in the industrial important strain *Monascus purpureus* SM001. *Metab. Eng*, **12**(1), 1-7.

Jones, M. G., 2007. The first filamentous fungal genome sequences: *Aspergillus* leads the way for essential everyday resources or dusty museum specimens? *Microbiology-(UK)*, **153**, 1-6.

Katayama, T., Tanaka, Y., Okabe, T., Nakamura, H., Fujii, W., Kitamoto, K., Maruyama, J., 2016. Development of a genome editing technique using the CRISPR/Cas9 system in the industrial filamentous fungus *Aspergillus oryzae*. *Biotechnol. Lett*, **38**(4), 637-642.

Keller, N. P., 2019. Fungal secondary metabolism: regulation, function and drug discovery. *Nat. Rev. Microbiol*, **17**(3), 167-180.

Kim, D., Ku, S., 2018. Beneficial effects of *Monascus* sp KCCM 10093 pigments and derivatives: A mini review. *Molecules*, **23**(1), 15.

Kim, H. J., Ji, G. E., Lee, I., 2007. Natural occurring levels of citrinin and monacolin K in Korean *Monascus* fermentation products. *Food Sci. Biotechnol*, **16**(1), 142-145.

Klimek, M., Wang, S., Ogunkanmi, A., 2009. Safety and efficacy of red yeast rice (*Monascus purpureus*) as an alternative therapy for hyperlipidemia. *P & T,* **34**(6), 313–327.

Koren, S., Walenz, B. P., Berlin, K., Miller, J. R., Bergman, N. H., Phillippy, A. M., 2017. Canu: scalable and accurate long-read assembly via adaptive k-mer weighting and repeat separation. *Genome Res*, **27**(5), 722-736.

Lee, C. L., Pan, T. M., 2012. Development of *Monascus* fermentation technology for high hypolipidemic effect. *Appl. Microbiol. Biotechnol*, **94**(6), 1449-1459.

Li, D. D., Tang, Y., Lin, J., Cai, W. W., 2017. Methods for genetic transformation of filamentous fungi. *Microb. Cell. Fact*, **16**, 13.

Li, J. T., Zhang, Y. H., Zhang, Y. C., Yu, P. L., Pan, H. Y., Rollins, J. A., 2018. Introduction of large sequence inserts by CRISPR-Cas9 to create pathogenicity mutants in the multinucleate filamentous pathogen *Sclerotinia sclerotiorum*. *mBio*, **9**(3), 19.

Lian, X. J., Liu, L. Z., Dong, S. R., Wu, H., Zhao, J. X., Han, Y. J., 2015. Two new *Monascus* red pigments produced by Shandong Zhonghui food company in China. *Eur. Food Res. Technol*, **240**(4), 719-724.

Liang, B., Du, X. J., Li, P., Sun, C. C., Wang, S., 2018. Investigation of citrinin and pigment biosynthesis mechanisms in *Monascus purpureus* by transcriptomic analysis. *Front. Microbiol*, **9**, 11.

Liao, J. K., 2002. Beyond lipid lowering: the role of statins in vascular protection. *Int. J. Cardiol*, **86**(1), 5-18.

Lin, C. C., Li, T. C., Lai, M. M., 2005. Efficacy and safety of *Monascus purpureus* Went rice in subjects with hyperlipidemia. *Eur. J. Endocrinol*, **153**(5), 679-686.

Lin, L., Wu, S. F., Li, Z. J., Ren, Z. Y., Chen, M. H., Wang, C. L., 2018. High expression level of *mok E* enhances the production of monacolin K in *Monascus*. *Food Biotechnol*, **32**(1), 35-46.

Lin, Y. L., Wang, T. H., Lee, M. H., Su, N. W., 2008. Biologically active components and nutraceuticals in the *Monascus*-fermented rice: a review. *Appl. Microbiol. Biotechnol*, **77**(5), 965-973.

Liu, L. J., Zhao, J. X., Huang, Y. L., Xin, Q., Wang, Z. L., 2018. Diversifying of chemical structure of native *Monascus* pigments. *Front. Microbiol*, **9**, 13.

Liu, Q., Gao, R. R., Li, J. G., Lin, L. C., Zhao, J. Q., Sun, W. L., Tian, C. G., 2017. Development of a genome-editing CRISPR/Cas9 system in thermophilic fungal *Myceliophthora* species and its application to hyper-cellulase production strain engineering. *Biotechnol. Biofuels*, **10**, 14.

Liu, Q. P., Xie, N. N., He, Y., Wang, L., Shao, Y. C., Zhao, H. Z., Chen, F. S., 2014. *MpigE*, a gene involved in pigment biosynthesis in *Monascus ruber* M7. *Appl. Microbiol. Biotechnol*, **98**(1), 285-296.

Liu, R., Chen, L., Jiang, Y. P., Zhou, Z. H., Zou, G., 2015. Efficient genome editing in filamentous fungus *Trichoderma reesei* using the CRISPR/Cas9 system. *Cell Discov*, **1**, 11.

Ma, J. Y., Li, Y. G., Ye, Q., Li, J., Hua, Y. J., Ju, D. J., Zhang, D. C., Cooper, R., Chang, M., 2000. Constituents of red yeast rice, a traditional Chinese food and medicine. *J. Agric. Food Chem*, **48**(11), 5220-5225.

Matsu-ura, T., Baek, M., Kwon, J., Hong, C., 2015. Efficient gene editing in *Neurospora crassa* with CRISPR technology. *Fungal Biol Biotechnol*, **2,** 4.

Meyer, V., Andersen, M.R., Brakhage, A.A., Braus G.H., Caddick, M.X., Cairns T.C., de Vries, R.P., Haarmann, T., Hansen, K., Hertz-Fowler, C., Krappmann, S., Mortensen, U.H., Penalva, M.A., Ram, A.F.J. Head, R.M., 2016. Current challenges of research on filamentous fungi in relation to human welfare and a sustainable bio-economy: a white paper. *Fungal Biol Biotechnol*, **3**, 6.

Nagy, G., Szebenyi, C., Csernetics, A., Vaz, A.G., Tóth, E., Vágvölgyi, C., Papp, T., 2017. Development of a plasmid free CRISPR-Cas9 system for the genetic modification of *Mucor circinelloides*. *Sci Rep* **7**, 16800.

Nielsen, M. L., Isbrandt, T., Rasmussen, K. B., Thrane, U., Hoof, J. B., Larsen, T. O., Mortensen, U. H., 2017. Genes linked to production of secondary metabolites in *Talaromyces atroroseus* revealed using CRISPR-Cas9. *PLoS One*, **12**(1), 9.

Nodvig, C. S., Hoof, J. B., Kogle, M. E., Jarczynska, Z. D., Lehmbeck, J., Klitgaard, D. K., Mortensen, U. H., 2018. Efficient oligo nucleotide mediated CRISPR-Cas9 gene editing in *Aspergilli*. *Fungal Genet. Biol*, **115**, 78-89.

Nodvig, C. S., Nielsen, J. B., Kogle, M. E., Mortensen, U. H., 2015. A CRISPR-Cas9 system for genetic engineering of filamentous fungi. *PLoS One*, **10**(7), 18.

Patakova, P., 2013. *Monascus* secondary metabolites: production and biological activity. *J. Ind. Microbiol. Biotechnol*, **40**(2), 169-181.

Pohl, C., Kiel, J., Driessen, A. J. M., Bovenberg, R. A. L., Nygard, Y., 2016. CRISPR/Cas9 based genome editing of *Penicillium chrysogenum. ACS Synth. Biol*, **5**(7), 754-764.

Sakai, K., Kinoshita, H., Nihira, T., 2009. Identification of *mokB* involved in monacolin K biosynthesis in *Monascus pilosus*. *Biotechnol. Lett*, **31**(12), 1911-1916.

Salazar-Cerezo, S., Kun, R. S., de Vries, R. P., Garrigues, S., 2020. CRISPR/Cas9 technology enables the development of the filamentous ascomycete fungus *Penicillium subrubescens* as a new industrial enzyme producer. *Enzyme Microb. Technol*, **133**, 8.

Sanger, F., Nicklen, S., Coulson, A. R., 1977. DNA sequencing with chain-terminating inhibitors. *Proc. Natl. Acad. Sci. U. S. A*, **74**(12), 5463-5467.

Sansbury, B. M., Hewes, A. M., Kmiec, E. B., 2019. Understanding the diversity of genetic outcomes from CRISPR-Cas generated homology-directed repair. *Commun. Biol*, **2**, 10.

Schuster, M., Kahmann, R., 2019. CRISPR-Cas9 genome editing approaches in filamentous fungi and oomycetes. *Fungal Genet. Biol*, **130**, 43-53.

Schuster, M., Schweizer, G., Kahmann, R., 2018. Comparative analyses of secreted proteins in plant pathogenic smut fungi and related basidiomycetes. *Fungal Genet. Biol*, **112**, 21-30.

Shi, T. Q., Gao, J., Wang, W. J., Wang, K. F., Xu, G. Q., Huang, H., Ji, X. J., 2019. CRISPR/Cas9-based genome editing in the filamentous fungus *Fusarium fujikuroi* and its application in strain engineering for gibberellic acid production. *ACS Synth. Biol,* **8**(2), 445-454.

Shi, T. Q., Liu, G. N., Ji, R. Y., Shi, K., Song, P., Ren, L. J., Huang, H., Ji, X. J., 2017. CRISPR/Cas9-based genome editing of the filamentous fungi: the state of the art. *Appl. Microbiol. Biotechnol*, **101**(20), 7435-7443.

Shimizu, T., Kinoshita, H., Ishihara, S., Sakai, K., Nagai, S., Nihira, T., 2005. Polyketide synthase gene responsible for citrinin biosynthesis in *Monascus purpureus*. *Appl. Environ. Microbiol*, **71**(7), 3453-3457.

Slater, E. E., Macdonald, J. S.,1988. Mechanism of action and biological profile of HMG CoA reductase inhibitors – a new therapeutic alternative. *Drugs*, **36**, 72-82.

Smits, T. H. M., 2019. The importance of genome sequence quality to microbial comparative genomics. *BMC Genomics*, **20**(1), 4.

Song, R. J., Zhai, Q., Sun, L., Huang, E. X., Zhang, Y., Zhu, Y. L., Guo, Q. Y., Tian, Y. A., Zhao, B. Y., Lu, H., 2019. CRISPR/Cas9 genome editing technology in filamentous fungi: progress and perspective. *Appl. Microbiol. Biotechnol*, **103**(17), 6919-6932.

Turgeon, B. G., Condon, B., Liu, J., Zhang, N., 2010. Protoplast transformation of filamentous fungi. *Methods in molecular biology (Clifton, N.J.)*, **638**, 3–19.

Van Tieghem, M., 1884. *Monascus*, Genre Nouveau De L'Ordre Des Ascomycétes, *Bulletin de la Société Botanique de France*, **31**(5), 226-231.

Wang, Q., Cobine, P. A., Coleman, J. J., 2018. Efficient genome editing in *Fusarium oxysporum* based on CRISPR/Cas9 ribonucleoprotein complexes. *Fungal Genet. Biol*, **117**, 21-29.

Ward, N. C., Watts, G. F., Eckel, R. H., 2019. Statin toxicity mechanistic insights and clinical implications. *Circ.Res*, **124**(2), 328-350.

Weber, J., Valiante, V., Nodvig, C. S., Mattern, D. J., Slotkowski, R. A., Mortensen, U. H., Brakhage, A. A., 2017. Functional reconstitution of a fungal natural product gene cluster by advanced genome editing. *ACS Synth. Biol,* **6**(1), 62-68.

Wen, Q. Y., Cao, X. H., Chen, Z. T., Xiong, Z. X., Liu, J. H., Cheng, Z. X., Zheng, Z. H., Long, C. N., Zheng, B. D., Huang, Z. W., 2020. An overview of *Monascus* fermentation processes for monacolin K production. *Open Chem*, **18**(1), 10-21.

Wenderoth, M., Pinecker, C., Voss, B., Fischer, R., 2017. Establishment of CRISPR/Cas9 in *Alternaria alternata*. *Fungal Genet. Biol*, **101**, 55-60.

Weyda, I., Yang, L., Vang, J., Ahring, B. K., Lubeck, M., Lubeck, P. S., 2017. A comparison of Agrobacterium-mediated transformation and protoplast-mediated transformation with CRISPR-Cas9 and bipartite gene targeting substrates, as effective gene targeting tools for *Aspergillus carbonarius*. *J. Microbiol. Methods*, **135**, 26-34.

Whon, T. W., Chung, W. H., Lim, M. Y., Song, E. J., Kim, P. S., Hyun, D. W., Shin, N. R., Bae, J. W., Nam, Y. D., 2018. Data descriptor: The effects of sequencing platforms on phylogenetic resolution in 16 S rRNA gene profiling of human feces. *Sci. Data*, **5,** 15.

Wistreich, G.A., 2007. *Microbiology perspectives: a photographic survey of the microbial world*. Pearson Education.

Xie, N. N., Liu, Q. P., Chen, F. S., 2013. Deletion of *pigR* gene in *Monascus ruber* leads to loss of pigment production. *Biotechnol. Lett*, **35**(9), 1425-1432.

Yang, Y., Liu, B., Du, X. J., Li, P., Liang, B., Cheng, X. Z., Du, L. C., Huang, D., Wang, L., Wang, S., 2015. Complete genome sequence and transcriptomics analyses reveal pigment biosynthesis and regulatory mechanisms in an industrial strain, *Monascus purpureus* YY-1. *Sci Rep* **5**, 9.

Zhang, C., Meng, X. H., Wei, X. L., Lu, L., 2016. Highly efficient CRISPR mutagenesis by microhomology-mediated end joining in *Aspergillus fumigatus*. *Fungal Genet. Biol*, **86**, 47-57.

Zheng, Y. M., Lin, F. L., Gao, H., Zou, G., Zhang, J. W., Wang, G. Q., Chen, G. D., Zhou, Z. H., Yao, X. S., Hu, D., 2017. Development of a versatile and conventional technique for gene disruption in filamentous fungi based on CRISPR-Cas9 technology. *Sci Rep* **7**, 10.

Zhao, B. Y., Lu, H., 2019. CRISPR/Cas9 genome editing technology in filamentous fungi: progress and perspective. *Appl. Microbiol. Biotechnol*, **103**(17), 6919-6932.

Abstract in Korean

홍국균은 인간의 건강에 긍정적인 영향을 주는 식품 보조제로 오랜 기간 동안 사용되고 있다. 홍국균이 생산하는 대표적인 2차 대사산물은 모나콜린 케이, 홍국색소, 시트리닌이 있다. 모나콜린 케이는 스타틴으로써 HMG-CoA 환원효소로 간에서 합성되는 콜레스테롤 합성을 억제하여 고지혈증 치료제로 사용된다. 홍국색소는 단백질과의 착색력이 좋아 식품의 천연색소로서 다양한 산업에서 널리 이용되고 있다. 또한, 홍국색소는 천연색소 기능뿐만 아니라 항염 및 항산화 효과가 있다고 알려져 왔고 건강기능식품으로도 주목받았다.

본 논문에서는 PacBio SMRT 시퀀싱 기술을 기반으로 한국 전통 장류 식품에서 분리한 *M. ruber*의 홍국색소 생산량을 높이기 위해 CRISPR/Cas9 시스템을 적용하였다. Chapter 2에서는 PacBio RSII 시퀀서와 *de novo* 어셈블리를 사용하여 총 길이 25.9 Mb로 이루어진 *M. ruber*의 유전체를 얻었다. PacBio SMRT 시퀀싱을 통해서 얻어낸 어셈블리 결과, *M. ruber*는 9,639개의 유전자를 포함한 13개의 contig로 구성되어 있었다. 2차 대사산물에 관여하는 유전자를 분석한 결과, 시트리닌 합성 유전자는 대부분 손실되었고, 유익한 2차 대사산물인 모나콜린 케이와 홍국색소 유전자가 존재하였다, 이는 *M. ruber*가 시트리닌 생산이 없는 유망한 산업 균주로 사용될 수 있다는 것을 나타낸다. Citrinin 생성 유무를 정확히 확인하기 위해 HPLC 분석을 수행하였고, 최종적으로 *M. ruber*에서 citrinin이 검출되지 않았다.

Chapter 3에서는 negative regulator로 추정되는 *MpigI*와 *MpigI'*에 CRISPR/Cas9 시스템을 적용하였다. 효과적인 유전자 교정으로

mutation을 유도하기 위해 두 개의 sgRNA를 타겟 유전자에 상보적인 염기서열로 설계했다. 플라스미드 벡터로 운반된 Cas9과 *in vitro*로 합성된 sgRNAs는 형질전환을 통해 타겟 유전자를 교정했다. Sanger 시퀀싱 결과를 바탕으로 최종적으로 6개의 mutants가 생성되었다. Mutation이 유도된 *M. rube*가 wild-type에 비해 홍국색소 생산성이 높아진 것을 확인하였다. Mutants에 대한 추가 분석을 통해 CRISPR/Cas9 시스템이 *M. ruber*에서 성공적으로 구축되었음을 검증했다. 본 연구는 *M. ruber*의 CRISPR/Cas9 시스템에 대한 첫 번째 연구이다.